Interference Mitigation for Reverse Spectrum Sharing in B5G/6G Satellite-Terrestrial Networks

Hao-Wei Lee, Chun-Chia Chen, Stephanie Liao, Abdelkader Medles, Debby Lin, I-Kang Fu, Hung-Yu Wei

***Abstract*—Satellite and terrestrial network (TN) convergence is an important trend to offer truly ubiquitous worldwide coverage in the B5G/6G era. Based on the recently published 3GPP Rel-17 Non-Terrestrial Network (NTN) specifications, the industry is actively driving commercialization and enabling satellite connection over the cellular phone. However, the spectrum shortage problem will become more severe after satellite services broadly penetrate consumer markets. Spectrum sharing between satellite and cellular networks is a promising solution to mitigate the spectrum shortage problem. However, it will inevitably result in severe interference across two systems if not properly managed. We propose a novel interference mitigation technique that jointly considers the satellite network with earth-fixed beamforming capability and the cellular network. The proposed Interference-aware radio resource group sharing mechanism combined with sub-optimal TN and NTN grouping algorithm optimizes the overall system capacity. It also ensures the signal quality over each link operates at an acceptable level. The mechanism demonstrates the feasibility of NTN-TN spectrum sharing and outperforms the baselines with 94% to 138% capacity utility, which is contributed by enhanced 72% TN available bandwidth and 45% to 133% NTN throughput.**

***Index Terms*—Satellite-terrestrial network, NTN-TN spectrum sharing, radio resource allocation, interference mitigation**

I. Introduction

Spectrum sharing between satellite and terrestrial networks would enhance spectral efficiency and is critical in the B5G/6G network. The B5G/6G network is anticipated to deliver a broad coverage area and exceptional capacity, which is necessitated by the proliferation of IoT devices and applications that require high throughput. An integrated satellite-terrestrial network, which complements the terrestrial's coverage gap and the satellite's low system capacity, is a promising B5G/6G network architecture [1]. Sharing the spectrum between satellite and terrestrial networks can enhance both networks' capacity and utilization [2].

There is a risk of inter-system interference that could severely impact both networks despite the benefits of spectrum sharing between satellite and terrestrial networks. Thus, it is crucial to mitigate interference to implement spectrum sharing successfully. A recent study [3] suggests that reverse pairing is a promising interference mitigation technique for satellite-terrestrial spectrum sharing. This technique involves the terrestrial network (TN) transmitting in the opposite direction to the non-terrestrial network (NTN) in a frequency-division duplexing (FDD) band. However, the results also note that the NTN uplink (UL) still experiences a significant signal-to-interference plus noise ratio (SINR) decrease in reverse pairing due to interference from the TN.

In this research, we aim to optimize the TN's capacity while maintaining a decent throughput for NTN UL. We focus on addressing a spectrum sharing scenario that involves a low Earth orbit (LEO) satellite network and numerous cellular networks within the extreme coverage of NTN. Both NTN and TN provide mobile services with handheld devices. Due to the mobility of the LEO satellite, we consider the achieved NTN UL throughput and the available spectrum of TN base stations (BSs) as NTN's and TN's utility, respectively, to evaluate the capacity of the NTN-TN network. We propose an interference-aware radio resource group sharing mechanism based on design principles inspired by observations of preliminary simulations. The mechanism involves dividing NTN user equipments (UEs), radio resources, and TN BSs into groups and mapping them to resource groups. We formulate the NTN-TN spectrum sharing via the proposed mechanism as a capacity optimization problem, which is solved using the proposed population-based sub-optimal TN and NTN grouping algorithm. The contributions of the research are as follows:

- To the best of our knowledge, we are the first researchers to investigate spectrum sharing with a large-scale NTN-TN network (consider more than ten thousand BSs) rigorously. Through extensive simulations using a 3GPP-calibrated simulator, we identify the NTN UL as the most vulnerable victim link in NTN-TN spectrum sharing. Our simulation results also reveal that TNs outside an NTN beam's coverage may still cause severe interference with NTN UL, highlighting the need to consider all TNs within NTN coverage as potential interference sources.
- We propose an interference-aware radio resource group sharing mechanism based on reverse pairing, a static interference mitigation method. The proposed mechanism allows TNs to utilize the common spectrum while maintaining the NTN UL throughput, which is achieved by dividing the NTN UEs and TN BSs into groups and then mapping these groups to radio resource groups. By considering TN available bandwidth and NTN UL throughput jointly, we formulate radio resource allocation in the

Hung-Yu Wei and Hao-Wei Lee are grateful for the funding support from Mediatek under grant MTKC-2023-1050. (Corresponding author: Hung-Yu Wei)

Hao-Wei Lee is with Graduate Institute of Communication Engineering, National Taiwan University, Taipei 10617, Taiwan (e-mail: D06942009@ntu.edu.tw).

Chun-Chia Chen, Chen-I Stephanie Liao, Abdelkader Medles, Debby Lin, and I-Kang Fu are with MediaTek Inc., Hsinchu City 300, Taiwan (e-mail: {Cc.Alanchen, Stephanie.Liao, kader.medles, Debby.Lin, ik.fu}@mediatek.com).

Hung-Yu Wei is with the Department of Electrical Engineering and Graduate Institute of Communication Engineering, National Taiwan University, Taipei 10617, Taiwan (e-mail: hywei@ntu.edu.tw).

© 2024 IEEE. Personal use of this material is permitted. Permission from IEEE must be obtained for all other uses, in any current or future media, including reprinting/republishing this material for advertising or promotional purposes, creating new collective works, for resale or redistribution to servers or lists, or reuse of any copyrighted component of this work in other works.

NTN-TN network as a capacity optimization problem.

- We propose optimal grouping conditions for NTN UEs and TN BSs and a sub-optimal TN and NTN grouping algorithm to solve the capacity optimization problem. The NTN UEs and TN BSs optimal grouping conditions first reduce the search space of the capacity optimization problem. The sub-optimal TN and NTN grouping algorithm then finds local optimal solutions within a limited number of iterations.
- We verify the feasibility and superiority of NTN-TN spectrum sharing via the proposed group sharing mechanism, showing an overall capacity improvement of 94% to 138%. Compared with baseline scenarios, the mechanism improves 72% TN available bandwidth and 45% to 133% NTN throughput.

This paper is organized as follows. Related works are listed in section II. NTN-TN architecture, preliminary simulation, and the most vulnerable victim link identification are provided in section III. We introduce the proposed interference-aware radio resource group sharing mechanism in section IV. The throughput model of the proposed group sharing mechanism is constructed in section VI. We formulate NTN-TN spectrum sharing as a capacity optimization in section VII. Sections VIII and IX deliver two optimal grouping conditions and the proposed sub-optimal TN and NTN grouping algorithms, respectively. Section X shows simulation results and the analyses to verify the superiority of the proposed group sharing method. Finally, section XI concludes this work.

II. Related Work

Studies on joint radio resource and interference mitigation for spectrum sharing in satellite-terrestrial networks can be categorized into three main areas: (1) cooperation mechanisms between NTN and TN [4]–[12], (2) cognitive spectrum utilization for satellite-terrestrial integrated networks [13]–[19], and (3) Non-orthogonal multiple access (NOMA) terrestrial-satellite networks [20]–[25].

The investigation of cooperation mechanisms between satellite and terrestrial networks typically involves the application of game theory to analyze or optimize these mechanisms [4]–[12]. A multi-channel cooperative spectrum sharing mechanism based on Vickrey-Clarke-Groves (VCG) was proposed for a satellite-terrestrial IoT network in [4]. Authors in [7] consider a cooperation scenario where a primary satellite network coexists with multiple secondary terrestrial networks.

The cognitive spectrum satellite-terrestrial network papers investigated the application of cognitive radio to enable spectrum sharing between satellite and terrestrial networks [13]–[19]. In [13], satellite networks operate as a secondary system to explore the available spectra without causing harmful interference to the terrestrial network. The authors in [14] propose a joint radio resource allocation scheme with non-ideal spectrum sensing consideration to minimize the end-to-end delay of the secondary satellite network.

The papers on NOMA terrestrial-satellite networks [20]–[25] investigate the potential of interference cancellation technology to improve spectral efficiency. The first paper [20] examines the spectrum allocation for access and backhaul links in a network where satellite and terrestrial UEs use NOMA technology to share the spectrum of the access link. The terrestrial BSs connect to the satellite through backhaul links.

Limited research exists on joint radio resource and interference management in mobile satellite service and mobile networks. Most prior work in NTN-TN spectrum sharing focuses on different network types (e.g., NTN internet-of-things (IoT) and TN IoT, fixed satellite services, and mobile networks), neglecting the spectrum sharing between mobile satellite services and mobile networks.

Also, the prior studies often underestimate the impact of aggregated inter-system interference power on NTN, failing to consider the significant influence of numerous TN BSs and terrestrial UEs within NTN's coverage. Managing thousands of TN BSs using the mechanisms and algorithms presented in state of the art is infeasible or inefficient due to the increased complexity. Therefore, this study addresses joint radio resource and interference management for a satellite-terrestrial network, considering a more practical number of interference sources within NTN's extreme coverage for ubiquitous mobile service.

III. System Architecture and Victim Link Identification in NTN-TN Spectrum Sharing

This section first provides the proposed system architecture of NTN-TN spectrum sharing and then discusses the compatibility between 3GPP NTN architecture and our proposed architecture. Section III-C presents the preliminary simulation results to justify the proposed architecture. Further, based on the preliminary simulation results, we identify the most vulnerable victim links and provide the interference power distribution from the BS to the satellite to verify the necessity of the proposed reference signal design.

A. System Architecture of NTN-TN Spectrum Sharing

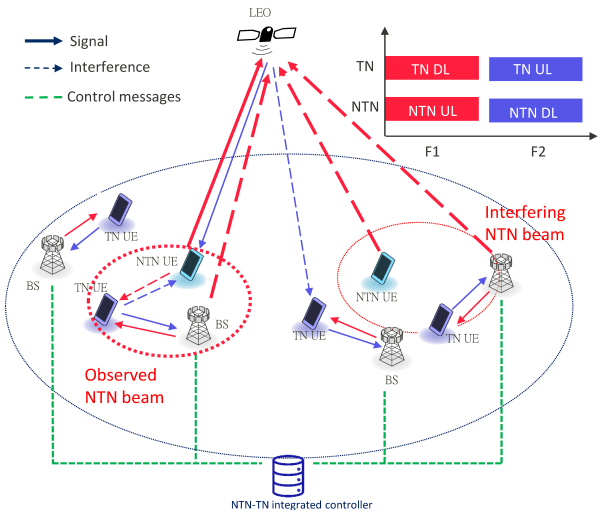

Fig. 1. System architecture of NTN-TN spectrum sharing. NTN and TN operate in FDD mode but in reverse pairing. The controller coordinates NTN and TN via resource allocation with the information provided by TN BS. The bold lines highlight the concentrated victim and aggressor links.

© 2024 IEEE. Personal use of this material is permitted. Permission from IEEE must be obtained for all other uses, in any current or future media, including reprinting/republishing this material for advertising or promotional purposes, creating new collective works, for resale or redistribution to servers or lists, or reuse of any copyrighted component of this work in other works.

Fig. 1 illustrates the system architecture of satellite-terrestrial spectrum sharing. The spectrum sharing scenario consists of an NTN and TNs. The NTN comprises a multi-beam LEO satellite and handheld UEs which connect to the satellite, i.e., NTN UEs. BSs and handheld UEs which connect to a BS, i.e., TN UEs, constitute TN networks.

The NTN and TNs operate in FDD mode in our studied architecture. Most satellite network operates in the FDD band since the long guard band due to long propagation in TDD would lower the spectral efficiency [26], [27]. Thus, we assume the terrestrial network would operate in FDD mode to share the FDD spectrum with NTN.

In our architecture, the NTN and TNs use the common FDD spectrum in a reverse direction. Reverse pairing is a novel and effective interference mitigation method for NTN-TN spectrum sharing. According to results in [3], NTN has a limited impact on TN, and the reverse pairing outperforms the normal pairing in NTN UL and downlink (DL). In NTN UL, the satellite receives less interference from TN in the reverse pairing due to the BS downtilt angle and directional antenna. In NTN DL, UEs follow maximum reference signal received power (RSRP) association, resulting in spatial isolation between NTN UEs and TN UEs. This isolation allows NTN UEs in the reverse pairing to achieve a higher average SINR than those in the normal pairing. NTN UEs are assumed to be full buffers and eager to obtain higher throughput since the below Mbps UL throughput provided by the current Rel-17's NR NTN falls below the requirements of most applications.

In light of the current limitations of Rel-17's NR NTN, which often results in UEs experiencing limited UL throughput below the Mbps range, the performance of various applications is hindered. Acknowledging this shortfall in UL throughput, we assume that NTN UEs operate with full buffers and endeavor to achieve higher throughput to meet the requirements of diverse applications.

An integrated controller for NTN-TN coordination plays an important role in improving spectral efficiency by effectively allocating resources based on essential TN and NTN information, including NTN UE UL received power and the propagation loss between the satellite and TN BSs. To estimate the propagation loss between the satellite and TN BSs, the controller periodically configures the satellite to broadcast a reference signal, which is then measured by the BSs. The measurement reports of the reference signal are sent to the controller upon request. Fig. 2 illustrates the detailed signal flow involved in the resource allocation process, visually representing the coordinated resource allocation mechanism in the integrated NTN-TN network.

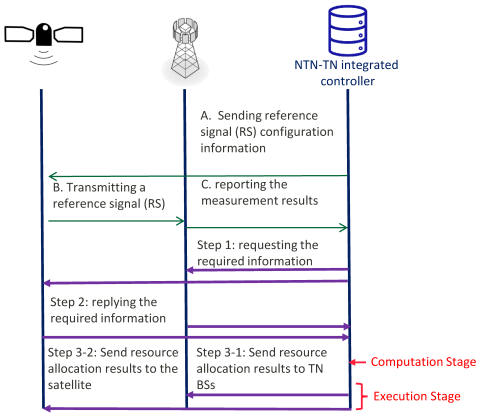

Fig. 2. Signal flow of reference signal configuration for BS interference measurement in the proposed system.

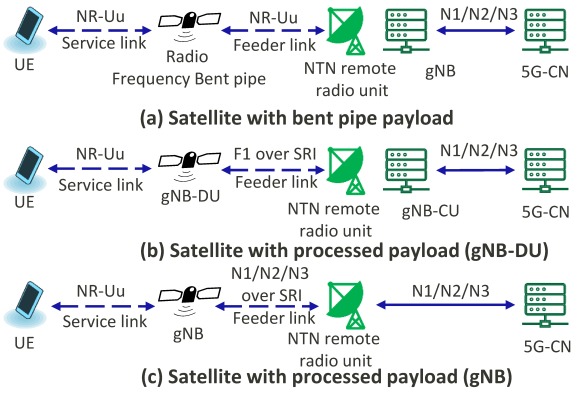

Fig. 3. RAN architecture options in non-terrestrial network considered in TR 38.811.

B. Compatibility to 3GPP NTN RAN architecture

In TR 38.811 [26], 3GPP analyzed the NTN radio access network (RAN) architecture using a satellite's either bent-pipe or processed payload. A bent-pipe payload involves radio frequency conversion, analog filtering, and amplification. In the bent-pipe architecture (Fig. 3(a)), NR RAN functions would be deployed at a gNB near the NTN remote radio unit. Due to satellites' power and mass limitations, a processed payload may not be able to implement all RAN functions. In this case, a processed payload with some RAN functions would correspond to a gNB-DU in NR. The F1 interface would be encapsulated by the satellite radio interface (SRI) to link the satellite and the gNB-CU (Fig. 3(b)). Conversely, a satellite with all RAN functions would operate as a gNB and connect to the 5G-CN throughput N1/N2/N3 interface encapsulated SRI (Fig. 3(c)).

The proposed method for spectrum sharing between NTN and TN is designed to accommodate both scenarios: a satellite with all gNB functions and a satellite implementing gNB-DU within the NTN RAN architecture. Additionally, the resource allocation of the group sharing mechanism can be communicated using RRC messages, specifically the *ServingCellConfig* in the *spCellConfig* via NR-Uu, allowing for reconfiguring of the operating frequency range of TN BSs.

C. Effectiveness and interference pattern on reverse pairing

We provide preliminary simulation results conducted by our 3GPP-calibrated simulator (introduced in section X-A). We compared the SINR in reverse pairing with the SINR in normal pairing and no sharing scenarios.

Fig. 4(a) shows the advantage of reverse pairing in NTN DL, owing to interference from BSs with high directional antenna gain is much higher than from UEs. Geographical separation

© 2024 IEEE. Personal use of this material is permitted. Permission from IEEE must be obtained for all other uses, in any current or future media, including reprinting/republishing this material for advertising or promotional purposes, creating new collective works, for resale or redistribution to servers or lists, or reuse of any copyrighted component of this work in other works.

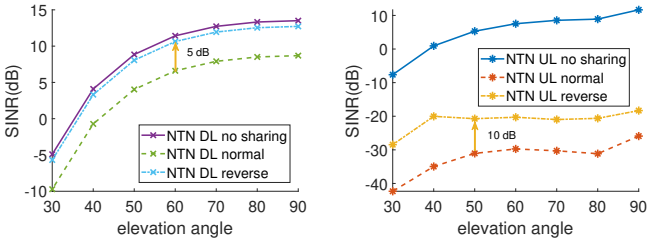

(a) NTN DL SINR is improved 5 dB by reverse pairing. (b) NTN UL SINR is improved 10 dB by reverse pairing.

Fig. 4. Result of NTN SINR in no sharing, reverse pairing, and normal pairing.

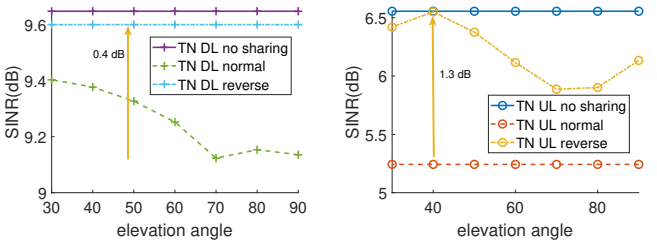

(a) TN DL SINR is improved 0.4 dB by reverse pairing. (b) TN UL SINR is improved 1.3 dB by reverse pairing.

Fig. 5. Result of TN SINR in no sharing, reverse pairing, and normal pairing.

between NTN UEs and TN UEs minimizes the degradation in DL SINR in reverse pairing. Conversely, DL SINR in NTN systems under normal pairing is 5-7 dB lower than in the no sharing scenario.

Fig. 4(b) shows that the reverse pairing yields a UL SINR 10 dB higher than the normal pairing. This superiority of the reverse pairing is because BSs' antenna directivity can efficiently reduce its interference to the satellite.

- Preliminary observation 1: The reverse pairing has less impact on NTN DL and UL.

Fig. 5 shows the TN average SINR in scenarios with normal, reverse, and no spectrum sharing. Firstly, in DL, both reverse and normal pairing achieve SINR levels that are close to the SINR without spectrum sharing. Secondly, in Fig. 5(b), the "TNUL reverse" has an SINR 0.3 dB lower than the SINR without spectrum sharing, while the "TNUL normal" has an SINR 1.3 dB lower than the SINR without spectrum sharing.

- Preliminary observation 2: NTN has a limited interference impact on TN.
- Preliminary observation 3: The reverse pairing outperforms the normal pairing in TN and NTN.

Fig. 1 highlights the concentrated NTN UL-TN DL sharing scenario with bold arrows. As highlighted in [3], NTN UL experiences the most significant SINR decrease in the reverse pairing compared to the no sharing scenario. Our preliminary simulation in Fig. 4(b) also shows that the average SINR of NTN UL falls below the minimum SINR required for normal mobile service operation, i.e., -10 dB, as defined in [28]. Thus, in reverse pairing, NTN UL and TN DL are identified as the most vulnerable victim and aggressor links, respectively.

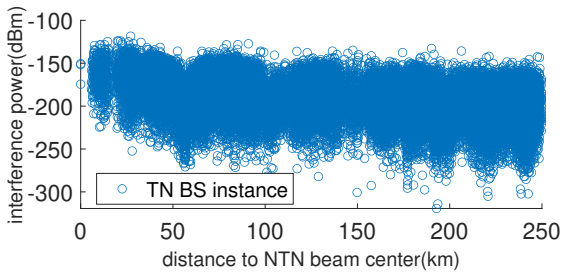

Fig. 6. TN BS to satellite interference power versus distance between TN BSs and the NTN beam center. The low correlation indicates that all BSs within the NTN coverage could potentially cause severe interference.

The low correlation of BS to satellite interference power and distance between BS and the NTN beam center shown in Fig. 6 implies that BSs far from the beam center could still cause severe interference to NTN UL. Consequently, an interference mitigation mechanism for NTN UL should consider all BSs in the NTN's coverage.

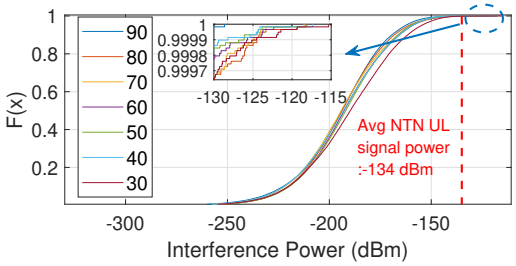

Fig. 7. Base station to satellite interference power CDF with elevation angles. The wide distribution of interference power and a tiny portion of BS with severe interference proves that NTN UL can share radio resources with most BSs regardless of elevation angle.

The wide distribution in Fig. 7 indicates that only a small percentage of BSs have dominant interference power. The dominant interference power is primarily caused by shadow fading and line-of-sight (LOS)/non-line-of-sight (NLOS) conditions, and these BSs are geographically loosely correlated (see Fig. 6). Thus, the proposed reference signal procedure, leveraging the broadcast advantages of NTN, is an efficient method for identifying BSs with dominant interference power.

Spectrum sharing between NTN and TN involves a trade-off between their respective capacities. One approach to improving NTN UL SINR is to prevent TN BSs with strong interference from sharing resources. However, this may limit the performance of those BSs, given the scarcity of available spectrum. Therefore, managing the capacity trade-off between NTN and TN requires careful consideration. In this work, we concentrate on radio resource sharing between NTN UL and TN DL in reverse pairing, as this is the area the greatest vulnerability exists.

IV. Interference-Aware Radio Resource Group Sharing Mechanism

We propose an interference-aware radio resource group sharing mechanism in this section. Firstly, we describe the NTN-TN network model and operation assumption. Section

© 2024 IEEE. Personal use of this material is permitted. Permission from IEEE must be obtained for all other uses, in any current or future media, including reprinting/republishing this material for advertising or promotional purposes, creating new collective works, for resale or redistribution to servers or lists, or reuse of any copyrighted component of this work in other works.

V-A delivers the group sharing mechanism design principles. Finally, we introduce the proposed group sharing mechanism and procedure steps.

V. NTN-TN NETWORK SYSTEM MODEL

We focus on the NTN UL-TN DL sharing scenario within the terrestrial-satellite network, as depicted in Fig. 1. In the satellite-terrestrial spectrum sharing scenario; there is a satellite with N_b NTN beams and N_{BS} TN BSs within the satellite's coverage area. When NTN and TN operate cooperatively, a UE selects the access node with the highest RSRP, which can either be the satellite or a TN BS. If a UE is within the coverage area of a TN BS, the RSRP received from TN would be greater than the RSRP received from NTN, leading to the UE connecting to NTN only when it is out of TN coverage. When a UE is outside the coverage of TN, it will select an NTN beam with the maximum RSRP to connect. In each NTN beam, assuming that more than N_{UE} UEs are outside of TN coverage, NTN schedules N_{UE} NTN UEs in the UL in a time slot to approximate intra-system interference. The common spectrum shared between NTN UL and TN DL has a bandwidth of λBMHz, where NTN adopts a frequency reuse factor of λ to mitigate intra-system interference, i.e., BMHz bandwidth for each NTN beam.

TABLE I
MATHEMATICAL NOTATIONS

Indices:	
N_b	number of NTN beams
N_{BS}	number of TN BSs
N_{UE}	number of NTN UEs in each NTN beam
M	number of radio resource groups
Sets:	
N_i^a	the set of NTN UEs in NTN group i of beam a
T_i	the set of TN BSs in TN group i
Parameters:	
B	bandwidth of an NTN beam
b_i	UL bandwidth of a NTN UE in group N_i^a
λ	NTN frequency reuse factor
P_t	TN BS transmission power density
η^{T_n,N_m^a}	power adjustment factor of a TN BS in group T_n to an NTN UE in group N_m^a
$I^{N_m^a}$	the aggregated intra-system interference to an NTN UE in group N_m^a
N_0	noise power
Variables:	
B_i	bandwidth of radio resource group i
I^{T_n,N_m^a}	aggregated interference power from TN BSs in group T_n to an NTN UE in group N_m^a
$\xi_j^{N_m^a}$	the SINR of an NTN UE j in group N_m^a
$\gamma_j^{N_m^a}$	the NTN UE j's spectral efficiency in group N_m^a
$\Gamma_j^{N_m^a}$	The NTN UE j's throughput in group N_m^a
U^T	TN's utility function
U^N	NTN's utility function
U	NTN-TN integrated network's utility function
Random variables:	
$L_{a,j}$	propagation loss between the satellite and ground unit j
$S_{a,i}^r$	interference power density of a TN BS i received at the NTN beam a
$P_{a,i}^{r,T_n}$	interference power of a BS i in group T_n received at NTN beam a
P_j^a	the received signal power at NTN beam a from NTN UE j
Decision variables:	
$x_k^{N_i^a}$	indication of whether NTN UE k is in group N_i^a
$x_{i,k}$	indication of whether TN BS k is in group T_i
$\boldsymbol{X}_n$	the set of group T_i's decision variables, $\boldsymbol{X}_n = \{x_{i,1}, .., x_{i,N_{BS}}\}$
$\boldsymbol{X}^{N_i^a}$	the set of group N_i^a's decision variables, $\boldsymbol{X}^{N_i^a} = \{x_1^{N_i^a}, .., x_{N_{UE}}^{N_i^a}\}$
δ_j^N	the upper received power threshold of group N_j^a
δ_j^T	the upper power density threshold of group T_j

A. Design Principles

The first design principle is to allocate more radio resources to TN BSs with lower interference levels. As demonstrated in Fig. 7, the interference power of many BSs has a minimal impact on NTN capacity. Thus, allowing those BSs to share more radio resources can effectively enhance the overall capacity as the capacity of TN is improved, and the impact on NTN capacity is negligible.

The second design principle is to share the radio resources utilized by an NTN UE with higher received signal power with more BSs. Signals with higher received power can resist more interference power. Thus, allowing more BSs to share the radio resources used by an NTN UE with higher received signal power can enhance TN capacity without significantly impacting the UE's throughput.

The third design principle is to assign more radio resources to NTN UEs with higher received signal power to compensate for the decrease in NTN capacity caused by the first and second design principles.

The last design principle is to allocate dedicated radio resources for the TN BSs that cause the most interference in order to safeguard the NTN UL from severe interference. As illustrated in Fig. 7, some BSs generate interference power that overwhelms all NTN received signal power. By allocating dedicated resources to these BSs, they can operate without causing detrimental effects on NTN capacity.

B. Steps of Group Sharing Mechanism

The following steps outline the proposed mechanism.

- Step 1: The total N_{UE} NTN UEs are assigned into $M-1$ groups, i.e., $N_{UE} = \sum_{i=1}^{M-1} |N_i|$. A radio resource unit b_i is allocated to an NTN UE in the group N_i, $i \in \mathbb{N}_{M-1}$, where $b_i \leq b_j, \forall i < j$.
- Step 2: The total BMHz radio resource is partitioned into M groups according to the number of UEs and radio resource units of NTN UE groups, i.e., $B = \sum_{i=1}^{M} B_i$ and $B_i = \|N_i\| b_i$. The resource group i of B_iMHz is allocated to the NTN UEs in N_i, $i \in \mathbb{N}_{M-1}$.
- Step 3: The total N_{BS} TN BSs are classified into M groups, i.e., $N_{BS} = \sum_{i=1}^{M} |T_i|$, in which the TN BSs in T_1 causes the least total interference, the TN BSs in T_2 causes more interference than the TN BSs in T_1, and so on. The TN BSs in T_M cause the most interference. Furthermore, the resource allocation for the TN BS in T_i is denoted by B_{T_i}, where $B_{T_i} = \sum_{j=i}^{M} B_j, i \in \mathbb{N}_M$.

In the first step, the total N_{UE} NTN UEs are partitioned into $M-1$ groups based on the second and third design principles. NTN UEs in the group N_i^a are assigned the same radio resource b_i. Moreover, to maintain the throughput of an NTN UE suffering from more interference from TN BSs, more radio resources should be allocated to it, that is, $b_i \leq b_j, \forall i < j$.

© 2024 IEEE. Personal use of this material is permitted. Permission from IEEE must be obtained for all other uses, in any current or future media, including reprinting/republishing this material for advertising or promotional purposes, creating new collective works, for resale or redistribution to servers or lists, or reuse of any copyrighted component of this work in other works.

The indication variable $x_k^{N_i^a} = 1$ indicates that NTN UE k belongs to group N_i^a; otherwise (i.e., $x_k^{N_i^a} = 0.$), NTN UE k does not belong to group N_i^a. The members of group N_i^a can be further defined as $N_i^a = \{k | x_k^{N_i^a} = 1\}$.

In the third step, the total N_{BS} TN BSs are partitioned into M groups based on the first and fourth design principles. The BSs in TN group T_i are allowed to operate on radio resource group i to group M. Consequently, all radio resources (i.e., B MHz) are allocated to a group of TN BSs that cause the least interference, which is designated as group T_1. Additionally, the TN BSs with the strongest interference power are assigned to group T_M and can only use the resource group M, which is reserved exclusively for TN. A binary variable $x_{i,k} \in \{0, 1\}$ is used to indicate whether a TN BS k belongs to group T_i or not, where $x_{i,k} = 1$ represents inclusion and $x_{i,k} = 0$ represents exclusion. The members of group T_i can be further defined as $T_i = \{k | x_{i,k} = 1\}, k \in \mathbb{N}_{N_{BS}}$.

In summary, all NTN UEs within an NTN group will be assigned the same radio resources and be affected by the same interference. Furthermore, the bandwidth of each resource group i can be determined by $B_i = |N_i| b_i, i \in \mathbb{N}_{M-1}$, where $B_M = B - \sum_{i=1}^{M-1} B_i$. Fig. 8 illustrates the proposed group sharing mechanism.

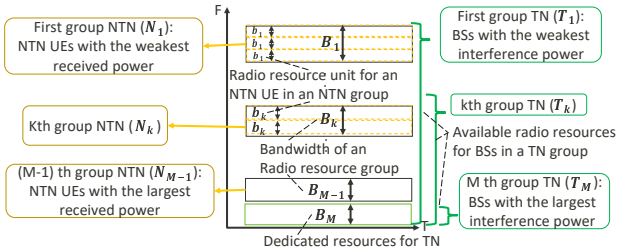

Fig. 8. Proposed mechanism: Interference-aware resource group sharing mechanism

VI. SINR AND THROUGHPUT MODEL IN PROPOSED RESOURCE GROUP SHARING MECHANISM

This section constructs the SINR and throughput model of NTN UL of the proposed mechanism step by step. Then the following subsections sequentially present the TN to NTN interference model and the intra-NTN interference model to construct the NTN SINR in the Interference-aware radio resource group sharing mechanism.

A. Non-terrestrial Propagation Model

The propagation loss $L_{a,j}$ between the satellite and a NTN UE j consists of free space path loss $\omega_{a,j}(d_{a,j}, f_c)$, shadow fading loss $SF_{a,j}$, and clutter loss $CL_{a,j}(\theta_j^e, f_c)$.

$$L_{a,j} = \omega_{a,j}(d_{a,j}, f_c) + SF_{a,j}(\theta_e) + CL_{a,j}(\theta_j^e, f_c) \quad (1)$$

$d_{a,j}$ stands for the distance between the NTN UE j and the satellite. The shadow fading loss $SF_{a,j}$ is modeled as a random variable that follows a log-normal distribution. When expressed in dB, the shadow fading variable follows a normal distribution $N(0, \sigma(\theta_j^e)^2)$, with a variance $\sigma(\theta_j^e)$ related to NTN UE j's elevation angle θ_j^e to the satellite.

The clutter loss $CL_{a,j}(\theta_j^e, f_c)$ models the attenuation of signal power due to surrounding buildings and objects on the ground. $CL_{a,j}(\theta_j^e, f_c)$ is related to the NTN UE j's elevation angle θ_j^e and the carrier frequency f_c.

B. Terrestrial DL to Non-terrestrial UL Interference Model

The following introduces the aggregated TN interference suffered by NTN UL of UEs in different NTN groups. The interference power density $S_{a,i}^r$ of a TN BS i received at the NTN beam a of the satellite can represent as

$$S_{a,i}^r = P_t G_i^t(\phi_{a,i}^H, \phi_{a,i}^V) L_{a,i} G_a^r(\theta_{a,i}), \quad (2)$$

where P_t indicates the TN BS transmission power density. The TN BS transmitter antenna gain to the satellite G_i^t is determined by the horizontal TN BS beam off-axis angle $\phi_{a,i}^H$ and the vertical TN BS beam off-axis angle $\phi_{a,i}^V$ to the satellite. $L_{a,i}$ expresses the propagation loss between TN BS i and the satellite. The satellite's receiver antenna gain $G_a^r(\theta_{a,i})$ to TN BS i is decided by the beam off-axis angle $\theta_{a,i}$ from the beam center of NTN beam a to TN BS i. The interference power of a BS in group T_n received at NTN beam a is

$$P_{a,i}^{r,T_n} = S_{a,i}^r \sum_{j=n}^{M} B_j. \quad (3)$$

Because a TN BS's DL bandwidth partially overlaps with an NTN UE's UL bandwidth, only a fraction of TN BS's interference power affects the NTN UL operation. In addition, we assume the interference power uniformly distributes in the allocated bandwidth b_m. Based on the assumptions, we here introduce a power adjustment factor η^{T_n, N_m^a} based on power density to model the fraction of affecting interference power from a TN BS in group T_n to an NTN UE in group N_m^a.

$$\eta^{T_n, N_m^a} = \begin{cases} \frac{b_m}{\sum_{j=n}^{M} B_j}, n \le m \\ 0, n > m \end{cases} \quad (4)$$

Regarding the $n \le m$ scenario, the interference power density of a TN BS in group T_n is written as $\frac{P_{a,i}^{r,T_n}}{\sum_{j=n}^{M} B_j}$. The multiplication of the interference power density and allocated UL bandwidth b_m can obtain the interference power that affects NTN UL in group N_m^a, which can be expressed as $\frac{P_{a,i}^{r,T_n}}{\sum_{j=n}^{M} B_j} b_m$. Therefore, the power adjustment factor $\eta^{T_n, N_m^a} = \frac{b_m}{\sum_{j=n}^{M} B_j}$ when $n \le m$. Regarding the scenario where $n > m$, the allocated bandwidth of a TN BS in group T_n does not overlap with that of an NTN UE in group N_m^a. Consequently, $\eta^{T_n, N_m^a} = 0$ when $n > m$.

The aggregated interference power from TN BSs in group T_n to an NTN UE in group N_m^a can be further indicated as

$$I^{T_n, N_m^a}(\boldsymbol{X}_n) = \sum_{i=1}^{N_{BS}} x_{n,i} P_{a,i}^{r,T_n} \eta^{T_n, N_m^a}, \quad (5)$$

where $\boldsymbol{X}_n = \{x_{n,i} | i \in \mathbb{N}_{N_{BS}}\}$.

© 2024 IEEE. Personal use of this material is permitted. Permission from IEEE must be obtained for all other uses, in any current or future media, including reprinting/republishing this material for advertising or promotional purposes, creating new collective works, for resale or redistribution to servers or lists, or reuse of any copyrighted component of this work in other works.

C. NTN Intra-system Interference Model

This subsection presents the approximate inter-beam interference experienced by the NTN UL of UEs in different NTN groups. The received interference of beam a at the satellite composes of inter-system interference and intra-system interference. The intra-system interference originates from NTN UEs in other beams using the same radio resources. Suppose an NTN UE j in group N_m^a of beam a uses radio resources overlapping the radio resources used by group $N_m^{\tilde{a}}$ of beam $\tilde{a}$. The interference power of an NTN UE $\tilde{j}$ in $N_m^{\tilde{a}}$ to the NTN UE j in UL can be expressed as

$$P_{j,\tilde{j}}^{a,\tilde{a}} = P_{\tilde{j}}^t G_{\tilde{j}}^t L_{a,\tilde{j}} G_a^r(\theta_{a,\tilde{j}}), \tag{6}$$

where $P_{\tilde{j}}^t$ denotes the UL transmission power of the NTN UE $\tilde{j}$, and $G_{\tilde{j}}^t$ represents the transmitter antenna gain. $L_{a,\tilde{j}}$ expresses the NTN UE $\tilde{j}$'s propagation loss to the satellite, and the NTN UE $\tilde{j}$ to beam a's off-axis angle $\theta_{a,\tilde{j}}$ determines the beam a's receiver antenna gain $G_a^r(\theta_{a,\tilde{j}})$.

We approximate the NTN intra-system interference with the interference power on average over NTN UEs in beam $\tilde{a}$. The computation of the interference power from group $N_m^{\tilde{a}}$ to the NTN UE j in UL requires group $N_m^{\tilde{a}}$'s radio resource allocation information, which could be hard to obtain. Consequently, we use the average interference power over NTN UEs in group $N_m^{\tilde{a}}$ to model the intra-system interference from group $N_m^{\tilde{a}}$ to the NTN UE j.

$$P_j^{a,\tilde{a}} = \frac{1}{|N_m^{\tilde{a}}|} \sum_{\tilde{j} \in N_m^{\tilde{a}}} P_{j,\tilde{j}}^{a,\tilde{a}} \tag{7}$$

We introduce a variable $\chi_{a,\tilde{a}} \in \{0, 1\}$ to express if the radio resources an NTN beam $\tilde{a}$ utilized overlap with the one used by the NTN beam a under a frequency reuse policy. The aggregated intra-system interference to an NTN UE j in group N_m^a can be written as

$$I^{N_m^a} = \chi_{a,\tilde{a}} \sum_{\tilde{a}=1, \tilde{a} \neq a}^{N_b} P_j^{a,\tilde{a}}. \tag{8}$$

D. SINR Model in NTN Groups of the Proposed Mechanism

The signal power received at the satellite from an NTN UE j served by an NTN beam a can be written as

$$P_j^a = P_j^t G_{t,j} L_{s,j} G_s(\theta_{a,j}), \tag{9}$$

where P_j^t is the NTN UE j's transmission power. $G_{t,j}$ represents NTN UE j's transmission antenna gain, $G_s(\theta_{a,j})$ states the satellite's receiver antenna gain with an NTN beam off-axis angle $\theta_{a,j}$. $L_{a,j}$ indicates the propagation loss between NTN UE j and the satellite. The SINR, denoted as ξ, of an NTN UE j associated with the satellite by NTN beam a in group N_m^a can be denoted as

$$\xi_j^{N_m^a}(\prod_{i=1}^{m} \boldsymbol{X}_i) = \frac{P_j^a}{\sum_{n=1}^{m} I^{T_n, N_m^a}(\boldsymbol{X}_n) + I^{N_m^a} + N_0}. \tag{10}$$

The throughput with adaptive coding and modulation can be approximated by an attenuated α and truncated form of the Shannon bound according to TR 38.803 [29]. Let ξ_{min} and ξ_{max} denote the code set's minimum and the maximum SINR, respectively. The signal can not be decoded when the SINR is lower than ξ_{min}. Therefore, We introduce a Heaviside step function $H(x)$ to model the throughput when $\xi_j^{N_m^a} < \xi_{min}$.

$$H(x) = \begin{cases} 1, x \geq 0 \\ 0, x < 0 \end{cases} \tag{11}$$

According to TR 38.803 [29], the NTN UE j's spectral efficiency $\gamma_j^{N_m^a}$ in group N_m^a can be expressed as

$$\begin{aligned} &\gamma_j^{N_m^a}(\prod_{i=1}^{m} \boldsymbol{X}_i) = \\ &\alpha log_2(1 + min(\xi_j^{N_m^a}(\prod_{i=1}^{m} \boldsymbol{X}_i), \xi_{max}))H(\xi_j^{N_m^a} - \xi_{min}). \end{aligned} \tag{12}$$

The NTN UE j's throughput $\Gamma_j^{N_m^a}$ in group N_m^a consists of the UL bandwidth b_m and spectral efficiency $\gamma_j^{N_m^a}$.

$$\Gamma_j^{N_m^a}(\prod_{i=1}^{m} \boldsymbol{X}_i) = b_m \gamma_j^{N_m^a}(\prod_{i=1}^{m} \boldsymbol{X}_i) \tag{13}$$

VII. Capacity Optimization Formulation

This section formulates the resource allocation of the proposed NTN-TN spectrum sharing mechanism as an optimization problem. We first introduce a utility function to represent the capacity of NTN-TN spectrum sharing. The capacity optimization through the proposed mechanism is formulated as non-linear programming in Section VII-B.

A. Capacity Utility in NTN-TN Spectrum Sharing

We sequentially introduce the capacity utility function of TN and NTN and then construct the capacity utility function of NTN-TN spectrum sharing.

We consider the BS's available bandwidth on average as the TN's utility. Due to the real-time coordination difficulty caused by the long propagation delay and NTN's extreme coverage, we consider a quasi-static spectrum sharing mechanism. The visible time of a LEO satellite at 600km altitude is about 12 minutes. A radio resource allocation result could be valid in about tens of seconds since the relative positions of the satellite and the BSs have only minor changes. During the valid duration, the environment of a BS could change. For instance, during the valid period, the propagation loss between BS and serving UEs might change, UEs might join or leave a BS, or BS could receive new service requests. Moreover, given its robustness in NTN-TN spectrum sharing, it is more meaningful to assess TN utility in terms of bandwidth rather than throughput. Consequently, we consider the BS's available bandwidth as a BS's utility. The TN's utility function U^T could be constructed by the sum of all BS's available bandwidth.

A TN BS in group T_n can utilize $\sum_{k=n}^{M} B_k$ bandwidth. The total bandwidth of all TN BSs in group T_n can be denoted as $\sum_{i=1}^{N_{BS}} x_{n,i} \sum_{k=n}^{M} B_k$. The TN network's utility U^T, which takes all group's total bandwidth on average, is indicated as

$$U^T(\prod_{i=1}^{M} \boldsymbol{X}_i) = \frac{1}{N_{BS}} \sum_{n=1}^{M} \sum_{i=1}^{N_{BS}} x_{n,i} \sum_{k=n}^{M} B_k. \tag{14}$$

© 2024 IEEE. Personal use of this material is permitted. Permission from IEEE must be obtained for all other uses, in any current or future media, including reprinting/republishing this material for advertising or promotional purposes, creating new collective works, for resale or redistribution to servers or lists, or reuse of any copyrighted component of this work in other works.

Regarding NTN's utility, we take the throughput sum of NTN beam a in UL as NTN's utility U^N. Firstly, the throughput accurately captures the vulnerability of NTN UL in the coexistence scenario. Furthermore, given the wide coverage of an NTN cell, the environment within the cell remains relatively stable during the valid duration. As a result, we deem the aggregated throughput of an NTN beam to be a suitable representative metric.

$$U^N(\prod_{i=1}^{M} \boldsymbol{X}_i \prod_{j=1}^{M-1} \boldsymbol{X}^{N_j^a}) = \sum_{j=1}^{M-1} \sum_{k \in N_j^a} \Gamma_k^{N_j^a} (\prod_{i=1}^{j} \boldsymbol{X}_i). \quad (15)$$

To guarantee utility product-based fairness between NTN and TN, we construct the utility function U from the product of the TN's utility U^T and the NTN's utility U^N to represent the capacity of the NTN-TN spectrum sharing.

$$U(\prod_{i=1}^{M} \boldsymbol{X}_i \prod_{j=1}^{M-1} \boldsymbol{X}^{N_j^a}) = U^T(\prod_{i=1}^{M} \boldsymbol{X}_i) U^N(\prod_{i=1}^{M} \boldsymbol{X}_i \prod_{j=1}^{M-1} \boldsymbol{X}^{N_j^a}) \quad (16)$$

In summary, we delve into the distinct characteristics of NTN UL vulnerability and TN DL robustness in the NTN-TN spectrum sharing scenario. Because of these performance discrepancies, utilizing different metrics for NTN and TN evaluations is essential. Although these metrics represent different physical variables, their combination comprehensively assesses the overall system performance. By considering the aggregate throughput of an NTN beam alongside the total bandwidth of TN BSs, we effectively capture the collective performance of both NTN and TN systems in a meaningful and holistic manner.

B. Capacity Utility Optimization

Problem ($\boldsymbol{P}$)

$$\max_{\boldsymbol{X}, \boldsymbol{X}^N} U(\boldsymbol{X}_1, ..., \boldsymbol{X}_M, \boldsymbol{X}^{N_1^a}, ..., \boldsymbol{X}^{N_{M-1}^a})$$

$$\text{s.t.} \quad \sum_{i=1}^{M} B_i = B \quad (17a)$$

$$B_j = b_j \sum_{i=1}^{N_{UE}} x_i^{N_j^a}, j \in \mathbb{N}_{M-1} \quad (17b)$$

$$\sum_{j=1}^{M} x_{j,i} = 1, i \in \mathbb{N}_{N_{BS}} \quad (17c)$$

$$x_{j,i} \in \{0,1\}, i \in \mathbb{N}_{N_{BS}}, j \in \mathbb{N}_M \quad (17d)$$

$$\sum_{j=1}^{M-1} x_i^{N_j^a} = 1, i \in \mathbb{N}_{N_{UE}} \quad (17e)$$

$$x_i^{N_j^a} \in \{0,1\}, i \in \mathbb{N}_{N_{UE}}, j \in \mathbb{N}_{M-1} \quad (17f)$$

(17) gives the formulation of capacity maximization through the proposed interference-aware radio resource group sharing mechanism, where the decisions in the mechanism are UEs and BSs group assignment. (17a) denotes the bandwidth sum of M non-overlapping radio resource equals the total bandwidth, and (17b) implies that the number of NTN UE in group N_j^a and the guaranteed per UE bandwidth b_j determines the bandwidth of j radio resource block. The notation $\mathbb{N}_k$ represents the set of positive integers less than k. (17c) and (17d) imply a TN BS should be in one TN group. (17e) and (17f) state an NTN UE should be in one NTN group.

VIII. Complexity Reduction by Optimal Grouping Conditions

Problem $\boldsymbol{P}$ is a non-linear integer programming (NIP) that is NP-hard ($(M-1)^{N_{UE}} M^{N_{BS}}$ feasible points). Thus, the time complexity of problem $\boldsymbol{P}$ grows exponentially with the number of BS and NTN UE. Because of the NTN's broad coverage, the BS number could range from one thousand to ten thousand, causing problem $\boldsymbol{P}$ to be computationally intractable. This section proposes two theorems of NTN's and TN's optimality grouping conditions which describe the grouping characteristics of an optimal solution to reduce search space and introduce a transformed problem $\boldsymbol{P}(\boldsymbol{\delta})$ with fewer dimensions of decision variables.

A. NTN and TN Optimal Grouping Conditions

NTN: To potentially increase the NTN UL throughput, allocating more radio resources to an NTN UE may be necessary. In particular, an NTN UE belonging to group N_j^a would be assigned a larger bandwidth b_j than an NTN UE in group N_i^a if $j > i$. However, the larger bandwidth also means that the NTN UE in group N_j^a would experience more interference from BSs in groups $Ti+1$ to T_j. This additional interference can reduce the potential benefits of allocating more radio resources. Thus, assigning an NTN UE with a stronger received signal power to an NTN group with a larger radio resource unit can be a viable solution to increase NTN's utility since those UE are more resistant to interference. Based on this observation, we establish an optimality condition for grouping NTN UEs.

Theorem 1. *Given any fixed* $\{\boldsymbol{X}_1, ..., \boldsymbol{X}_M\}$. *Suppose* $b_i \leq b_j, \forall i < j$. *If* $N_1^a, ..., N_{M-1}^a$ *are parts of a optimal solution, where* $N_j^a = \{i | x_i^{N_j^a} = 1\}$, *then* $\max_{i \in N_j^a} P_i^a < \min_{i \in N_{j+1}^a} P_i^a, \forall j \in \mathbb{N}_{M-2}$ *must hold.*

The proof of Theorem 1 is provided in Appendix A. According to Theorem 1, a threshold δ exists in the range of $\max_{i \in N_j^a} P_i^a$ and $\min_{i \in N_{j+1}^a} P_i^a$, i.e., $\max_{i \in N_j^a} P_i^a \leq \delta \leq \min_{i \in N_{j+1}^a} P_i^a$. Thus, the optimal assignment of NTN UEs into $M-1$ groups can be determined by the received signal power of NTN UEs and $M-2$ thresholds $\delta_1^N, ..., \delta_{M-2}^N$. The followings give the reformulation of the NTN UE groups.

$$\begin{aligned} N_1^a(\delta_1^N) &= \{i | E[P_i^a] \leq \delta_1^N\} \\ N_j^a(\delta_{j-1}^N, \delta_j^N) &= \{i | \delta_{j-1}^N < E[P_i^a] \leq \delta_j^N\}, 2 \leq j \leq M-2 \\ N_{M-1}^a(\delta_{M-2}^N) &= \{i | \delta_{M-2}^N < E[P_i^a]\} \end{aligned} \quad (18)$$

TN: Allocating more available bandwidth to BSs can increase TN's utility. Particularly, a BS belonging to group T_m would be assigned a larger bandwidth $\sum_{k=m}^{M} B_k$ than a BS in group T_n if $m < n$. However, a BS in group T_m would cause more interference to NTN UEs than a BS in group T_n. Thus, assigning a BS with lower interference power density to a

© 2024 IEEE. Personal use of this material is permitted. Permission from IEEE must be obtained for all other uses, in any current or future media, including reprinting/republishing this material for advertising or promotional purposes, creating new collective works, for resale or redistribution to servers or lists, or reuse of any copyrighted component of this work in other works.

TN group with more available bandwidth may increase TN's utility with only minor effects on NTN's utility. Accordingly, we establish an optimality condition for grouping BSs.

Theorem 2. *Given any fixed* $\{\boldsymbol{X}^{N_1^a}, ..., \boldsymbol{X}^{N_{M-1}^a}\}$ *and* $b_j \leq b_{j+1}$*, if* $T_1, ..., T_M$ *are parts of an optimal solution to problem* (P)*, where* $T_j = \{i | x_{j,i} = 1\}$*, then* $\max_{i \in T_j} S^r_{a,i} < \min_{i \in T_{j+1}} S^r_{a,i}, \forall j \in \mathbb{N}_M$ *must hold.*

The proof of Theorem 2 is provided in Appendix B. According to Theorem 2, a threshold δ exists between $\max_{i \in T_m} S^r_{a,i}$ and $\min_{i \in T_{m+1}} S^r_{a,i}$. Consequently, the optimal assignment of TN BSs into $M-1$ groups can be determined by the interference power density and $M-1$ thresholds $\delta^T_1, ..., \delta^T_{M-1}$. The reformulation of the BSs groups is expressed.

$$\begin{aligned} &T_1(\delta^T_1) = \{i | S^r_{a,i} \leq \delta^T_1\} \\ &T_j(\delta^T_{j-1}, \delta^T_j) = \{i | \delta^T_{j-1} < S^r_{a,i} \leq \delta^T_j\}, 2 \leq j \leq M-1 \\ &T_M(\delta^T_{M-1}) = \{i | \delta^T_{M-1} < S^r_{a,i}\} \end{aligned} \tag{19}$$

B. Reformulation with Optimal Conditions

According to Theorem 2, the interference power density and thresholds $\{\delta^T_1, ..., \delta^T_{M-1}\}$ could resolve the optimal group assignment of TN BSs. For convenience, the vector expressions of the decision variables are given.

$$\boldsymbol{\delta}^N = [\delta^N_1, ..., \delta^N_{M-2}]^T \tag{20a}$$

$$\boldsymbol{\delta}^T = [\delta^T_1, ..., \delta^T_{M-1}]^T \tag{20b}$$

(21) reformulates the TN's utility function.

$$\begin{aligned} U^T(\boldsymbol{\delta}^T) = \frac{1}{N_{BS}} (&\sum_{i \in T_1(\delta^T_1)} \sum_{k=1}^{M} B_k + \\ &\sum_{j=2}^{M-1} \sum_{i \in T_j(\delta^T_{j-1}, \delta^T_j)} \sum_{k=j}^{M} B_k + \sum_{i \in T_M(\delta^T_{M-1})} B_M) \end{aligned} \tag{21}$$

Additionally, the SINR of NTN UL in terms of $\{\delta^T_1, ..., \delta^T_{M-1}\}$ is given.

$$\xi_j^{N_m^a}(\delta^T_1, ..., \delta^T_m) = \frac{P^a_j}{I^{T_1, N_m^a}(\delta^T_1) + \sum_{n=2}^{m} I^{T_n, N_m^a}(\delta^T_{n-1}, \delta^T_n) + I^{N_m^a} + N_0} \tag{22}$$

The reformulated spectral efficiency $\gamma_j^{N_m^a}$ and the throughput $\Gamma_j^{N_m^a}$ derived from $\xi_j^{N_m^a}$ are expressed as the following.

$$\begin{aligned} &\gamma_j^{N_m^a}(\delta^T_1, ..., \delta^T_m) = \alpha log2(1 + min(\xi_j^{N_m^a}(\delta^T_1, ..., \\ &\delta^T_m), \xi_{max})) H(\xi_j^{N_m^a} - \xi_{min}) \end{aligned} \tag{23}$$

$$\Gamma_j^{N_m^a}(\delta^T_1, ..., \delta^T_m) = b_m \gamma_j^{N_m^a}(\delta^T_1, ..., \delta^T_m) \tag{24}$$

From Theorem 1, the received signal power and thresholds $\{\delta^N_1, ..., \delta^N_{M-2}\}$ could decide the optimal group assignment of NTN UEs. Thus, the reformulated NTN's utility is

$$\begin{aligned} U^N(\boldsymbol{\delta}^T, \boldsymbol{\delta}^N) = &\sum_{k \in N_1(\delta^N_1)} \Gamma_k^{N_1^a}(\delta^T_1) \\ &+ \sum_{j=2}^{M-2} \sum_{k \in N_j^a(\delta^N_{j-1}, \delta^N_j)} \Gamma_k^{N_j^a}(\delta^T_1, ..., \delta^T_j) + \\ &\sum_{k \in N_{M-1}^a(\delta^N_{M-2})} \Gamma_k^{N_{M-1}^a}(\delta^T_1, ..., \delta^T_{M-1}). \end{aligned} \tag{25}$$

The capacity utility in terms of $\{\boldsymbol{\delta}^T, \boldsymbol{\delta}^N\}$ is

$$U(\boldsymbol{\delta}^T, \boldsymbol{\delta}^N) = U^T(\boldsymbol{\delta}^T) U^N(\boldsymbol{\delta}^T, \boldsymbol{\delta}^N). \tag{26}$$

For expression convenience, we introduce ordered sets $\hat{\boldsymbol{P}}^r_a = \{\hat{P}^r_{a,1}, ..., \hat{P}^r_{a,N_{UE}}\}$, which contains received signal power $P^r_{a,i}$ in ascending order, and $\hat{\boldsymbol{S}}^r_a = \{\hat{S}^r_{a,1}, ..., \hat{S}^r_{a,N_{BS}}\}$, which contains interference power density $S^r_{a,i}$ in ascending order.

The decision variables $\boldsymbol{\delta}^N$ and $\boldsymbol{\delta}^T$ can be viewed as discrete variables since the utility function changes only when the NTN or TN group members change. Let $\hat{P}^r_{a,j_1}$ and $\hat{P}^r_{a,j_2}$ be the minimum and maximum received signal power in group N_j, respectively. The members of an NTN group N_j would increase only when $\delta^N_{j-1} \leq \hat{P}^r_{a,j_1-1}$ or $\delta^N_j \geq \hat{P}^r_{a,j_2+1}$ and would decrease only when $\delta^N_{j-1} \geq \hat{P}^r_{a,j_1+1}$ or $\delta^N_j \leq \hat{P}^r_{a,j_2-1}$. Similar to NTN groups, TN groups have the property discussed above. Consequently, the decision variables $\delta^N_i \in \hat{\boldsymbol{P}}^r_a, i \in \mathbb{N}_{M-2}$ and $\delta^T_i \in \hat{\boldsymbol{S}}^r_a, i \in \mathbb{N}_{M-1}$.

Problem $(\boldsymbol{P}(\boldsymbol{\delta}))$

$$\max_{\boldsymbol{\delta}^T, \boldsymbol{\delta}^N} \quad U(\delta^T_1, ..., \delta^T_{M-1}, \delta^N_1, ..., \delta^N_{M-2})$$

$$\text{s.t.} \quad \sum_{i=1}^{M} B_i = B \tag{27a}$$

$$B_j = b_j \| N_j^a \|, j \in \mathbb{N}_{M-1} \tag{27b}$$

$$\delta^N_j \leq \delta^N_{j+1}, j \in \mathbb{N}_{M-3} \tag{27c}$$

$$\min_{i \in \mathbb{N}_{N_{UE}}} P^{r,T_n}_{a,i} \leq \delta^N_j, j \in \mathbb{N}_{M-2} \tag{27d}$$

$$\delta^N_j \leq \max_{i \in \mathbb{N}_{N_{UE}}} P^{r,T_n}_{a,i}, j \in \mathbb{N}_{M-2} \tag{27e}$$

$$\delta^T_j \leq \delta^T_{j+1}, j \in \mathbb{N}_{M-2} \tag{27f}$$

$$\min_{i \in \mathbb{N}_{N_{BS}}} S^r_{a,i} \leq \delta^T_j, j \in \mathbb{N}_{M-1} \tag{27g}$$

$$\delta^T_j \leq \max_{i \in \mathbb{N}_{N_{BS}}} S^r_{a,i}, j \in \mathbb{N}_{M-1} \tag{27h}$$

Through the substitution of $\{\boldsymbol{\delta}^N, \boldsymbol{\delta}^T\}$ for $\{\boldsymbol{X}_{\{1,...,M\}}, \boldsymbol{X}^{N_{\{1,...,M-1\}}^a}\}$, the reformulated problem $P(\delta)$ is given in (27). The constraints (27c) and (27f) are the basis of the optimal grouping structure according to Theorems 1 and 2. The feasible region of $\{\delta^N_1, ..., \delta^N_{M-2}\}$ are given by constraints (27d) and (27e). Constraints (27g) and (27h) deliver the feasible region of $\{\delta^T_1, ..., \delta^T_{M-1}\}$.

C. Complexity analysis

The proposed problem formulation in (27) falls under the class of polynomial-time solvable (P) problems when the number of groups is fixed. Specifically, solving the formulated problem involves selecting $(M-2)$ thresholds among the

© 2024 IEEE. Personal use of this material is permitted. Permission from IEEE must be obtained for all other uses, in any current or future media, including reprinting/republishing this material for advertising or promotional purposes, creating new collective works, for resale or redistribution to servers or lists, or reuse of any copyrighted component of this work in other works.

received power of UEs and $(M-1)$ thresholds among the power density of TN BSs, resulting in a total of $C_{M-2}^{N_{UE}} \cdot C_{M-1}^{N_{BS}}$ feasible points to consider.

However, it is crucial to note that despite this polynomial-time solvable, the objective function in problem (27) lacks convexity even with linear relaxation. This characteristic has a significant impact on the computation complexity of the proposed problem formulation, which is on the order of $O((N_{UE})^{M-2}(N_{BS})^{M-1})$. As a consequence, when the number of TN BSs increases, the time required to achieve the global optimum grows with the power of $(M-1)$.

The complexity analysis sheds light on the computational challenges associated with the proposed problem, particularly as the number of TN BSs expands. It highlights the need for efficient algorithms and heuristics to address the computational complexity and provide near-optimal solutions.

IX. Sub-optimal TN and NTN grouping algorithm

The reformulated problem $P(\delta)$ presents a significant challenge as it falls into the category of non-convex non-linear integer programming. This classification makes the problem non-differentiable and renders it intractable to find a global optimal solution using approaches reliant on derivatives.

Derivative-free optimization methods have emerged as valuable alternatives, seeking optimal solutions without relying on derivative information. Among these methods, local search algorithms offer a heuristic approach to tackling computationally challenging optimization problems. By iteratively exploring the search space and making local changes, the local search algorithm aims to converge toward an optimal solution within a predefined time limit. Building upon these insights, we propose a sub-optimal TN and NTN grouping algorithm based on local search to find a locally optimal solution.

However, even after applying linear relaxation, the objective function in problem $P(\delta)$ still lacks convexity. Consequently, the search space encompasses various local optimal points that can hinder the local search algorithm from reaching the global optimum. Our proposed algorithm augments the local search approach by incorporating an escape mechanism. This mechanism is designed to prevent the algorithm from becoming trapped at a local optimum by conditionally exploring new regions of the search space. By combining the effectiveness of local search with the flexibility of the escape mechanism, our algorithm mitigates the risk of converging to suboptimal solutions and increases the likelihood of discovering improved solutions.

In addition to incorporating the escape mechanism, our proposed algorithm also integrates a population-based search technique. Population-based search is a class of optimization methods that concurrently maintain and improve multiple candidate solutions. Motivated by the advantages of population-based searches, we enhance our proposed method by extending it to consider multiple candidate solutions simultaneously, aiming to approach a better local optimum.

In summary, our proposed algorithm tackles the problem $P(\delta)$, which is non-convex non-linear integer programming, by proposing a sub-optimal TN and NTN grouping algorithm. This algorithm incorporates an escape mechanism to overcome the presence of local optimal points. It also integrates a population-based search technique to enhance the exploration and exploitation of multiple candidate solutions.

A. Local search

In the local search phase, the algorithm iteratively updates the current exploratory point by selecting a neighboring point that yields an improved objective function value. To identify the neighbors of an exploratory point, we define the functions in (28) that determine the indices of δ_j^N within $\hat{\boldsymbol{P}}_a^r$ and δ_j^T within $\hat{\boldsymbol{S}}_a^r$.

$$\delta_j^{-N}(\hat{\boldsymbol{P}}_a^r) = i \quad \text{if} \quad \delta_j^N = \hat{P}_{a,i}^r \tag{28a}$$

$$\delta_j^{-T}(\hat{\boldsymbol{S}}_a^r) = i \quad \text{if} \quad \delta_j^T = \hat{S}_{a,i}^r \tag{28b}$$

Let $\boldsymbol{\delta} = [(\boldsymbol{\delta^N})^T, (\boldsymbol{\delta^T})^T]^T$. We define the distance functions d_k^N and d_k^T to measure the index distance of the kth element in $\boldsymbol{\delta^N}$ and $\boldsymbol{\delta^T}$, respectively.

$$\begin{aligned} d_k^N(\dot{\boldsymbol{\delta}}^N, \ddot{\boldsymbol{\delta}}^N) &= |\dot{\delta}_k^{-N}(\hat{\boldsymbol{P}}_a^r) - \ddot{\delta}_k^{-N}(\hat{\boldsymbol{P}}_a^r)| \\ d_k^T(\dot{\boldsymbol{\delta}}^T, \ddot{\boldsymbol{\delta}}^T) &= |\dot{\delta}_k^{-T}(\hat{\boldsymbol{S}}_a^r) - \ddot{\delta}_k^{-T}(\hat{\boldsymbol{S}}_a^r)| \end{aligned} \tag{29}$$

The set of neighbors $N(\dot{\boldsymbol{\delta}})$, including the exploratory point, for a given solution candidate $\dot{\boldsymbol{\delta}}$ is defined as

$$N(\dot{\boldsymbol{\delta}}) = \{\ddot{\boldsymbol{\delta}} | \max_k d_k^N(\dot{\boldsymbol{\delta}}^N, \ddot{\boldsymbol{\delta}}^N) \leq 1 \vee \max_k d_k^T(\dot{\boldsymbol{\delta}}^T, \ddot{\boldsymbol{\delta}}^T) \leq 1\}. \tag{30}$$

Once a new exploratory point is chosen, the algorithm updates the legacy exploratory point if the new one yields a better objective function value. The algorithm proceeds to the escape mechanism if a new exploratory point with a better objective function value does not exist.

B. Escape mechanism

To facilitate the escape mechanism, we introduce two parameters that assist in determining the escape.

$$\bar{U}^T(\boldsymbol{\delta}^T, \boldsymbol{\delta}^N) = \frac{U^T(\boldsymbol{\delta}^T, \boldsymbol{\delta}^N)}{U_{max}^T}, \bar{U}^N(\boldsymbol{\delta}^T, \boldsymbol{\delta}^N) = \frac{U^N(\boldsymbol{\delta}^T, \boldsymbol{\delta}^N)}{U_{max}^N} \tag{31}$$

U_{max}^T and U_{max}^N represent the TN and NTN's utility when exclusively using the spectrum, respectively. As such, U_{max}^T and U_{max}^N serve as upper bounds for the TN and NTN's utility, respectively. Consequently, $\bar{U}^T(\boldsymbol{\delta}^T, \boldsymbol{\delta}^N)$ and $\bar{U}^N(\boldsymbol{\delta}^T, \boldsymbol{\delta}^N)$ indicate the distances between the current utilities and their respective upper bounds. These parameters provide valuable information regarding which utility possesses a greater margin for improvement, ultimately aiding the exploration of alternative solutions.

The escape mechanism aims to determine the escape directions and corresponding step sizes when the search process becomes trapped in a local optimum point. We rely on the auxiliary parameters $\bar{U}^T(\boldsymbol{\delta}^T, \boldsymbol{\delta}^N)$ and $\bar{U}^N(\boldsymbol{\delta}^T, \boldsymbol{\delta}^N)$ to accomplish the purpose.

In **case A**, where $\bar{U}^T(\boldsymbol{\delta}^T, \boldsymbol{\delta}^N) \geq \bar{U}^N(\boldsymbol{\delta}^T, \boldsymbol{\delta}^N)$, the NTN utility possesses a greater potential for improvement. Consequently, decreasing the NTN's or TN's thresholds is the escape direction that can enhance the NTN utility.

© 2024 IEEE. Personal use of this material is permitted. Permission from IEEE must be obtained for all other uses, in any current or future media, including reprinting/republishing this material for advertising or promotional purposes, creating new collective works, for resale or redistribution to servers or lists, or reuse of any copyrighted component of this work in other works.

Decreasing NTN's thresholds $\boldsymbol{\delta}^N$: When an NTN threshold index $\boldsymbol{\delta}^N_{-j}$ decreases by s_N steps, the first s_N UEs with the strongest received signal power in group N^a_j are moved to group N^a_{j+1}. The change in the NTN utility can be expressed as

$$\begin{aligned} &U^N(\boldsymbol{\delta}^T, \boldsymbol{\delta}^{N'}|\boldsymbol{\delta}^{-N'} = \boldsymbol{\delta}^{-N} - s_N e_j) = U^N(\boldsymbol{\delta}^T, \boldsymbol{\delta}^N) + \\ &b_{j+1}\sum_{k=1}^{s_N}\gamma_k^{N^a_{j+1}}(\boldsymbol{\delta}^T) - b_j\sum_{k=1}^{s_N}\gamma_k^{N^a_j}(\boldsymbol{\delta}^T) \\ &= U^N(\boldsymbol{\delta}^T, \boldsymbol{\delta}^N) + \Delta U^N_j(s_N). \end{aligned} \tag{32}$$

Here, e_j represents the unit vector of the jth dimension. Moreover, the improvement in the NTN utility resulting from the threshold index transition from $\boldsymbol{\delta}^{-N'} = \boldsymbol{\delta}^{-N} - (s_N+1)e_j$ to $\boldsymbol{\delta}^{-N'} = \boldsymbol{\delta}^{-N} - s_N e_j$ can be denoted as

$$\Delta U^N_j(s_N+1) - \Delta U^N_j(s_N) = b_{j+1}\gamma^{N^a_{j+1}}_{n+1}(\boldsymbol{\delta}^T) - b_j\gamma^{N^a_j}_{n+1}(\boldsymbol{\delta}^T). \tag{33}$$

Since group N^a_{j+1} experiences more TN interference than N^a_j, and the received signal power is in decreasing order, the improvement in the NTN utility, $\Delta U^N_j(s_N+1) - \Delta U^N_j(s_N)$, decreases as s_N increases. As a result, there exists a largest improving step s^*_N that satisfies $\Delta U^N_j(s^*_N+1) - \Delta U^N_j(s^*_N) < 0$. Thus, to escape from the local optimum point and increase the NTN utility, we apply the new threshold index $\boldsymbol{\delta}^{-N'} = \boldsymbol{\delta}^{-N} - s^*_N e_j$, where e_j and s^*_N represent the escape direction and step size, respectively. By adjusting the NTN thresholds and judging by (33), the algorithm explores alternative solutions that offer improved NTN utility.

Decreasing TN's thresholds $\boldsymbol{\delta}^T$: When a TN threshold index $\boldsymbol{\delta}^T_{-j}$ decreases by s_T steps, the first s_T TN BSs with the strongest interference power in group T_j are moved to group T_{j+1}. As a result, the interference experienced by group N^a_j from the TN BSs decreases, leading to an increase in the NTN utility. In general, the NTN utility increases as the TN threshold index $\boldsymbol{\delta}^T_{-j}$ decreases.

However, the TN utility decreases as the TN threshold index $\boldsymbol{\delta}^T_{-j}$ decreases. Therefore, we aim to find an appropriate step size s_T that increases U^N and $\bar{U}^T\bar{U}^N$ along the improvement direction e_j. Consequently, (34) and (35) help us decide the escape direction and the largest improvement step.

$$\begin{aligned} &U^N(\boldsymbol{\delta}^{T'}|\boldsymbol{\delta}^{-T'} = \boldsymbol{\delta}^{-T} - (s_T+1)\boldsymbol{e}_j, \boldsymbol{\delta}^N) - \\ &U^N(\boldsymbol{\delta}^{T'}|\boldsymbol{\delta}^{-T'} = \boldsymbol{\delta}^{-T} - s_T\boldsymbol{e}_j, \boldsymbol{\delta}^N) \end{aligned} \tag{34}$$

$$\begin{aligned} &\bar{U}^T(\boldsymbol{\delta}^{T'}|\boldsymbol{\delta}^{-T'} = \boldsymbol{\delta}^{-T} - s^*_T\boldsymbol{e}_j, \boldsymbol{\delta}^N) \\ &\bar{U}^N(\boldsymbol{\delta}^{T'}|\boldsymbol{\delta}^{-T'} = \boldsymbol{\delta}^{-T} - s^*_T\boldsymbol{e}_j, \boldsymbol{\delta}^N) \le \\ &\bar{U}^T(\boldsymbol{\delta}^{T'}|\boldsymbol{\delta}^{-T'} = \boldsymbol{\delta}^{-T} - (s^*_T+1)\boldsymbol{e}_j, \boldsymbol{\delta}^N) \\ &\bar{U}^N(\boldsymbol{\delta}^{T'}|\boldsymbol{\delta}^{-T'} = \boldsymbol{\delta}^{-T} - (s^*_T+1)\boldsymbol{e}_j, \boldsymbol{\delta}^N) \end{aligned} \tag{35}$$

In **case B**(i.e., $\bar{U}^T(\boldsymbol{\delta}^T, \boldsymbol{\delta}^N) < \bar{U}^N(\boldsymbol{\delta}^T, \boldsymbol{\delta}^N)$), the TN utility has a greater potential for improvement. Increasing the NTN's thresholds or the TN's thresholds are the escape directions that can enhance the TN utility.

Increasing NTN's thresholds $\boldsymbol{\delta}^N$: When an NTN threshold index $\boldsymbol{\delta}^N_{-j}$ increases by s_N steps, the first s_N UEs with the weakest signal power in group N^a_{j+1} are moved to group N^a_j. This movement of the NTN threshold index leads to changes in the bandwidth allocation of the radio resource blocks j, $j+1$, and M, denoted as B_j, B_{j+1}, and B_M, respectively. The changes in the TN utility can be expressed as

$$\begin{aligned} &U^T(\boldsymbol{\delta}^T, \boldsymbol{\delta}^{N'}|\boldsymbol{\delta}^{-N'}) = U^N(\boldsymbol{\delta}^T, \boldsymbol{\delta}^N) + s_N b_j\sum_{i=1}^{j}|T_i| - \\ &s_N b_{j+1}\sum_{i=1}^{j+1}|T_i| + s_N(b_{j+1}-b_j)\sum_{i=1}^{M}|T_i| \\ &= U^N(\boldsymbol{\delta}^T, \boldsymbol{\delta}^N) - s_N b_{j+1}|T_{j+1}| + s_N(b_{j+1}-b_j)\sum_{i=j+1}^{M}|T_i|. \end{aligned} \tag{36}$$

The TN utility improvement through the adjustment of $\boldsymbol{\delta}^N_{-j}$ and s_N depends on the number of TN BSs in $T_{j+1}, \ldots, T_M$ and the values b_j, b_{j+1}. Therefore, we use (37) to determine the step sizes of an escape direction for the NTN's thresholds.

$$\begin{aligned} &U^T(\boldsymbol{\delta}^T, \boldsymbol{\delta}^{N'}|\boldsymbol{\delta}^{-N'} = \boldsymbol{\delta}^{-N} - (s_N+1)\boldsymbol{e}_j) - \\ &U^T(\boldsymbol{\delta}^T, \boldsymbol{\delta}^{N'}|\boldsymbol{\delta}^{-N'} = \boldsymbol{\delta}^{-N} - s_N\boldsymbol{e}_j) \le 0 \end{aligned} \tag{37}$$

Increasing TN's thresholds $\boldsymbol{\delta}^T$: When a TN threshold index $\boldsymbol{\delta}^T_{-j}$ increases by s_T steps, the first s_T TN BSs with the weakest interference power in group T_{j+1} are moved to group T_j. These s_T TN BSs can utilize additional bandwidth B_j of radio resource block j, resulting in an increase in the NTN utility as s_T increases.

However, as the TN BSs from T_j introduce more interference to group N^a_j, the NTN utility of group N^a_j decreases. Therefore, our goal is to find an appropriate step size s_T that increases U^T and $\bar{U}^T\bar{U}^N$ along the improvement direction e_j. Consequently, (38) and (39) help us decide the escape direction and the largest improvement step s^*_T.

$$\begin{aligned} &U^T(\boldsymbol{\delta}^{T'}|\boldsymbol{\delta}^{-T'} = \boldsymbol{\delta}^{-T} + (s_T+1)\boldsymbol{e}_j, \boldsymbol{\delta}^N) - \\ &U^T(\boldsymbol{\delta}^{T'}|\boldsymbol{\delta}^{-T'} = \boldsymbol{\delta}^{-T} + s_T\boldsymbol{e}_j, \boldsymbol{\delta}^N) \ge 0 \end{aligned} \tag{38}$$

$$\begin{aligned} &\bar{U}^T(\boldsymbol{\delta}^{T'}|\boldsymbol{\delta}^{-T'} = \boldsymbol{\delta}^{-T} + s_T\boldsymbol{e}_j, \boldsymbol{\delta}^N) \\ &\bar{U}^N(\boldsymbol{\delta}^{T'}|\boldsymbol{\delta}^{-T'} = \boldsymbol{\delta}^{-T} + s_T\boldsymbol{e}_j, \boldsymbol{\delta}^N) \le \\ &\bar{U}^T(\boldsymbol{\delta}^{T'}|\boldsymbol{\delta}^{-T'} = \boldsymbol{\delta}^{-T} + (s_T+1)\boldsymbol{e}_j, \boldsymbol{\delta}^N) \\ &\bar{U}^N(\boldsymbol{\delta}^{T'}|\boldsymbol{\delta}^{-T'} = \boldsymbol{\delta}^{-T} + (s_T+1)\boldsymbol{e}_j, \boldsymbol{\delta}^N) \end{aligned} \tag{39}$$

C. Sub-optimal grouping algorithm and complexity analysis

Algorithm 1 delivered the detailed sub-optimal TN and NTN grouping algorithm. Line 5 to 10 is the local search phase, and line 12 to 35 is the escape mechanism. In addition, we heuristically select the direction of maximum improvement as the escape direction. In light of the complexity analysis, the proposed algorithm targets the solution of the formulated problem (27) by selecting $(M-2)$ thresholds among the received power of UEs and $(M-1)$ thresholds among the power density of TN BSs. Consequently, the computational complexity of the proposed problem formulation scales with a time complexity of $O({N_{UE}}^{M-2}{N_{BS}}^{M-1})$. However, in order to strike a balance between computational feasibility and solution quality, the proposed algorithm is designed to identify a local optimal point within a maximum number of steps K_{max}.

By setting K_{max} to a value that is less than ${N_{UE}}^{M-2}{N_{BS}}^{M-1}$, the proposed algorithm aims to efficiently

© 2024 IEEE. Personal use of this material is permitted. Permission from IEEE must be obtained for all other uses, in any current or future media, including reprinting/republishing this material for advertising or promotional purposes, creating new collective works, for resale or redistribution to servers or lists, or reuse of any copyrighted component of this work in other works.

Algorithm 1 Sub-optimal TN and NTN grouping algorithm

for $i = 1 : N_{sample}$ **do**
  $K = 0$
  $\boldsymbol{\delta}_{i,K} = \boldsymbol{\delta}_{i,0}$
  while $K \leq K_{max}$ **do**
    $\tilde{\boldsymbol{\delta}} = \arg\max_{\boldsymbol{\delta} \in N(\boldsymbol{\delta}_{i,K})} U(\boldsymbol{\delta})$
    if $U(\boldsymbol{\delta}_{i,K}) < U(\tilde{\boldsymbol{\delta}})$ **then**
      $\boldsymbol{\delta}_{i,K+1} = \tilde{\boldsymbol{\delta}}$
      if $U(\boldsymbol{\delta}^i_{max}) < U(\tilde{\boldsymbol{\delta}})$ **then**
        $\boldsymbol{\delta}^i_{max} = \tilde{\boldsymbol{\delta}}$
      end if
    else
      $s_T = 1, s_N = 1$
      if $\bar{U}^T(\boldsymbol{\delta}^T_{i,K}, \boldsymbol{\delta}^N_{i,K}) \geq \bar{U}^N(\boldsymbol{\delta}^T_{i,K}, \boldsymbol{\delta}^N_{i,K})$ **then**
        $\tilde{\boldsymbol{e}}_j = \arg\max_{\{\boldsymbol{\delta}^N | \boldsymbol{\delta}^{-N} = \boldsymbol{\delta}^{-N}_{i,K} - \boldsymbol{e}_j\}} U^N(\boldsymbol{\delta}^T_{i,K}, \boldsymbol{\delta}^N)$
        while (33) ≥ 0 **do**
          $s_N = s_N + 1$
        end while
        $\boldsymbol{\delta}^{-N} = \boldsymbol{\delta}^{-N}_{i,k} - s_N \tilde{\boldsymbol{e}}_j$
        $\tilde{\boldsymbol{e}}_j = \arg\max_{\{\boldsymbol{\delta}^T | \boldsymbol{\delta}^{-T} = \boldsymbol{\delta}^{-T}_{i,K} - \boldsymbol{e}_j\}} U^N(\boldsymbol{\delta}^T, \boldsymbol{\delta}^N)$
        while (34) ≥ 0**and** (35) **do**
          $s_T = s_T + 1$
        end while
        $\boldsymbol{\delta}^{-T} = \boldsymbol{\delta}^{-T}_{i,k} - s_T \tilde{\boldsymbol{e}}_j$
      else
        $\tilde{\boldsymbol{e}}_j = \arg\max_{\{\boldsymbol{\delta}^N | \boldsymbol{\delta}^{-N} = \boldsymbol{\delta}^{-N}_{i,K} + \boldsymbol{e}_j\}} U^T(\boldsymbol{\delta}^T_{i,K}, \boldsymbol{\delta}^N)$
        while (37) ≥ 0 **do**
          $s_N = s_N + 1$
        end while
        $\boldsymbol{\delta}^{-N} = \boldsymbol{\delta}^{-N}_{i,k} + s_N \tilde{\boldsymbol{e}}_j$
        $\tilde{\boldsymbol{e}}_j = \arg\max_{\{\boldsymbol{\delta}^T | \boldsymbol{\delta}^{-T} = \boldsymbol{\delta}^{-T}_{i,K} - \boldsymbol{e}_j\}} U^N(\boldsymbol{\delta}^T, \boldsymbol{\delta}^N)$
        while (38) ≥ 0**and** (39) **do**
          $s_T = s_T + 1$
        end while
        $\boldsymbol{\delta}^{-T} = \boldsymbol{\delta}^{-T}_{i,k} + s_T \tilde{\boldsymbol{e}}_j$
      end if
    end if
    $K = K + 1$
  end while
end for
$\boldsymbol{\delta}^* = \arg\max_i U(\boldsymbol{\delta}^i_{max})$

converge towards a promising local optimal solution. While this approach does not guarantee finding the global optimum, it focuses on providing an effective solution with manageable computational complexity. This strategy ensures that the algorithm can be applied to real-world scenarios and deliver results in a timely manner.

X. Performance evaluation

In this section, we discuss the simulation experiments to verify the superiority of the proposed mechanism. We begin by introducing our 3GPP-calibrated simulator and baselines. Section X-B compares the capacity of group sharing with that of the baselines. To better understand how the group sharing mechanism offers a superior solution, we present a sequential analysis of the group sharing mechanism in the following subsections. It is important to note that the term "elevation angle," mentioned in the subsequent sections, refers to the angle between the observed NTN beam center and the satellite.

A. 3GPP-calibrated Simulator and Simulation Environment

A system-level simulator was constructed and calibrated against 3GPP TR 38.863 [28]. The scenario involves a steering-beam LEO satellite network operating at an altitude of 600km and cellular networks within the satellite's coverage area, which is a circular region with a 250km radius. This coverage area comprises both urban and rural regions. TN BSs are densely deployed with an inter-site distance (ISD) of 500m in urban areas and sparsely deployed with a minimum ISD of 5km in rural areas. The density of TN BSs is 0.1 BS/km^2, which is similar to the deployment density in Taiwan. The heights of urban and rural BSs are 25m and 35m, respectively. Two sets of group sharing parameters, $\{M = 3, b_1 = 2RB, b_2 = 3RB\}$ and $\{M = 4, b_1 = 2RB, b_2 = 3RB, b_3 = 4RB\}$, are selected for evaluation. In the observed NTN beam, there are 450 NTN UE devices, and 170 out of the 450 NTN UEs are randomly scheduled for UL transmission. The free space path loss $\omega(d, f_c)$ in dB for a distance d and a carrier frequency f_c is chosen from TR 38.901 [30].

$$\omega(d, f_c) = 32.45 + 20log10(f_c) + 20log(d) \tag{40}$$

We compare our proposed algorithm with three baseline scenarios for evaluating the performance of NTN-TN spectrum sharing. The first scenario is normal pairing, where NTN and TN operate in an FDD band with the same transmission direction. The second scenario is no sharing, where two resource blocks are allocated for each NTN UE, and the remaining radio resources are exclusively allocated to TN. Lastly, we utilize the TN BS sub-channel allocation method proposed in [31] as a benchmark for comparison, in which the NTN UL SINR is targeted at 5dB, as it represents the maximum utility, providing a reference point for evaluation.

In the "no sharing," the NTN-TN integrated controller allocates dedicated resources to NTN and TN, respectively. The controller first allocates two RBs for each scheduled NTN UE, allowing TN BSs to use any remaining radio resources not allocated to NTN. The detailed simulation parameters and models are listed in Table II.

B. Capacity Evaluation

Fig. 9 shows the utility of the proposed mechanisms with the proposed algorithm and baselines. The group sharing mechanisms with $M = 3$ and $M = 4$ show improved performances by 94% and 138%, respectively, compared to the baseline in [31]. Also, it is worth mentioning that normal pairing has zero throughputs since each UE has an SINR lower than the minimum operational required SINR of -10 dB.

Observation 1: The proposed group sharing has a 94% and 138% higher capacity utility than the baseline in [31] and no sharing.

Fig. 10(a) illustrates the average available bandwidth of the BSs. The proposed group sharing mechanism significantly improves the available bandwidth, with BSs achieving an additional 72% compared to no sharing. The slight decrease in available bandwidth with increasing elevation angles suggests that fewer BSs share the NTN resources due to the weaker NTN received signal power at lower elevation angles.

© 2024 IEEE. Personal use of this material is permitted. Permission from IEEE must be obtained for all other uses, in any current or future media, including reprinting/republishing this material for advertising or promotional purposes, creating new collective works, for resale or redistribution to servers or lists, or reuse of any copyrighted component of this work in other works.

TABLE II
SIMULATION PARAMETERS

number of NTN beams(N_b):	19
TN BS density	0.1 BS/km^2
number of TN BSs(N_{BS}):	58575
number of NTN UEs in each NTN beam(N_{UE}):	170
bandwidth of an NTN beam(B):	100MHz
NTN frequency reuse factor(λ)	3
TN BS transmission power density(P_t):	26 dBm/MHz
UE max transmission power:	23 dBm
noise power(N_0):	-144dBm
Satellite altitude	600km
NTN 3dB beam width	4.4 degree
Satellite Receiving max gain:	1.1 dBK^{-1}
BS transmission max gain(G^t):	24 dBi
Carrier frequency(f_c)	2GHz
inter-site distance (urban,rural):	500m,5000m
Satellite antenna pattern	TR 38.863 section 6.2.3.1
BS antenna panel model	TR 38.863 Table 6.2.3.2-1
BS donwtilt angle (urban,rural)	(10,3) degree
number of radio resource groups(M):	3,4
per UE UL bandwidth in group (b_1^N, b_2^N, b_3^N) :	(2RB,3RB,4RB)
attenuated parameter α	0.4
(ξ_{min}, ξ_{max})	(-10,22)
Maximum iteration K_{max}	10000

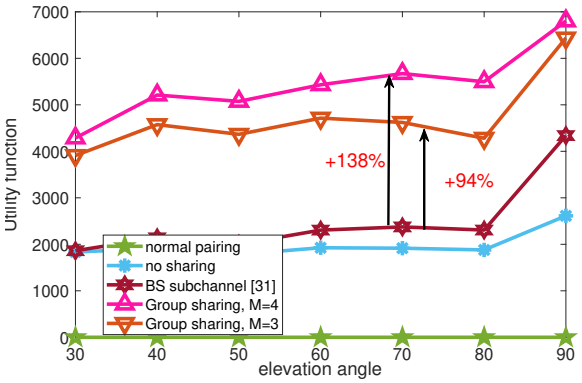

Fig. 9. Utility value comparison of group sharing and baselines. Group sharing improves at least 94% overall capacity from baselines.

Observation 2: BSs could achieve 72% more bandwidth in group sharing than in no sharing.

Observation 3: The group sharing with $M = 3$ is likely to achieve a higher TN BS bandwidth than with $M = 4$.

Fig. 10(b) presents a comparison of the overall NTN throughput. The group sharing mechanism with $M = 3$ results in a throughput improvement of 45% to 97% compared to baselines due to interference from TN BSs. Moreover, the group sharing mechanism with $M = 4$ settings has an NTN throughput enhancement of 71% to 133% than baselines, which is better than the $M = 3$ settings. Moreover, the NTN throughput of the group sharing mechanism remains steady with increasing elevation angles. Finally, it is worth mentioning that normal pairing has zero throughput since each UE has an SINR lower than the minimum operational required SINR of -10 dB.

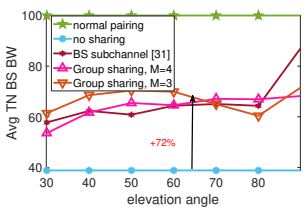

(a) Group sharing improves 72% TN BS bandwidth from no sharing.

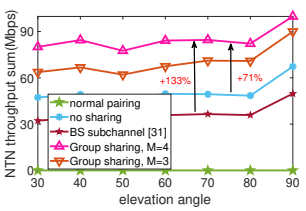

(b) Group sharing enhances at least 45% of the throughput of NTN UL from baselines.

Fig. 10. Results of TN and NTN capacity utility in group sharing and baselines.

Observation 4: The proposed mechanism has a 45% to 133% NTN throughput enhancement than baselines.

Observation 5: NTN throughput sum keeps steady along with the elevation angles in the group sharing.

Observation 6: The group sharing with $M = 4$ has a better NTN throughput than $M = 3$.

Based on observations 3 observations 6, a group sharing mechanism with a larger group number setting, i.e., a larger M, would offer a solution with higher NTN throughput and lower BS available bandwidth. Higher NTN throughput is because a larger M setting would provide more bandwidth to NTN UEs. However, providing more bandwidth to NTN UEs would reduce the available bandwidth of BSs with the strongest interference power, such as B_4 in group sharing $M = 4$, decreasing the average BS available bandwidth.

Observation 7: The group sharing mechanism with larger M settings would provide a solution of higher NTN throughput and lower BS available bandwidth.

Based on observation 7, a network operator could decide the radio resource group number M according to the NTN throughput and TN bandwidth preference.

C. SINR Improvement by Group Sharing Mechanism

Fig. 11 displays the average SINR of UEs in NTN groups that share resources. By combining reverse pairing and group sharing, the average SINR of UEs in group sharing with N_1 improves by 25 dB for $M = 3$ and $M = 4$, compared to normal pairing, but is still 10 dB lower than that of no sharing. Moreover, the SINR of N_2 in group sharing with $M = 3$ and N_3 in group sharing with $M = 4$, where N_2 and N_3 denote the groups that provide the largest radio resource unit to UEs, are close to the SINR of no sharing. The SINR difference between N_1 and $N_2(M = 3)/N_3(M = 4)$ suggests that group sharing would maintain the SINR of the group that provides the largest radio resource unit at a good level for high throughput while keeping N_1's SINR at a basic operational level to accommodate more TN BS's available spectrum.

Observation 8: The average SINR of the group sharing mechanism in the reverse pairing improves 25 ~ 40dB from the normal pairing.

Observation 9: The group sharing mechanism would keep the average SINR of NTN groups with more UL bandwidth units at a good level for high throughput and NTN groups with less UL bandwidth at a basic operation level for more TN BS's available spectrum.

Observations 4 and 9 provide valuable insights into the performance of the group sharing mechanism. The group sharing approach is observed to achieve an SINR level comparable to the no sharing scenario while significantly outperforming it in

© 2024 IEEE. Personal use of this material is permitted. Permission from IEEE must be obtained for all other uses, in any current or future media, including reprinting/republishing this material for advertising or promotional purposes, creating new collective works, for resale or redistribution to servers or lists, or reuse of any copyrighted component of this work in other works.

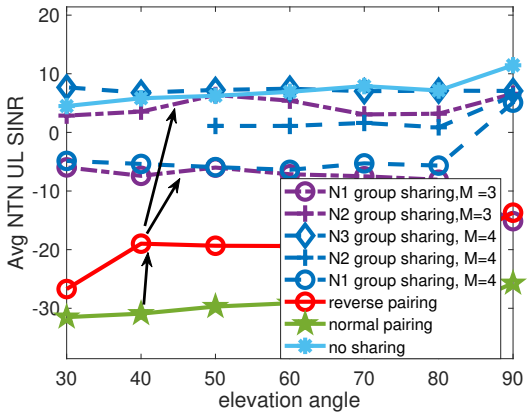

Fig. 11. NTN UE's SINR in group sharing, reverse pairing, and normal pairing. Reverse pairing first improves 10 dB NTN UL SINR from the normal pairing. Group sharing further improves 10 ~ 30 dB from reverse pairing.

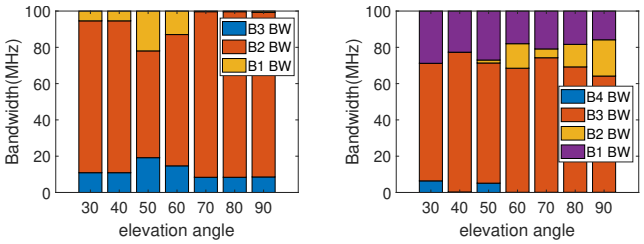

(a) Group sharing M=3 (b) Group sharing M=4

Fig. 12. Optimized radio resource group in different elevation angles. Group sharing adaptively increases the NTN group's threshold $\boldsymbol{\delta}^N$ as the elevation angle decreases.

terms of throughput. The key differentiating factor between group sharing and no sharing lies in the adaptive NTN UL radio resource allocation employed in group sharing. This allocation strategy, which considers the received signal power of UEs, contributes to the superior NTN UL throughput observed in the group sharing scenario.

Observation 10: The enhanced NTN UL throughput in group sharing can be attributed to the effective utilization of radio resources through adaptive NTN UL resource allocation.

D. Grouping Results Variation with Elevation Angle

Fig. 12 illustrates the relationship between the radio resource group's bandwidth, the number of UE in each group, and the elevation angles. The proposed mechanism aims to adaptively increase the thresholds of the NTN groups, denoted by $\boldsymbol{\delta}^N$, as the elevation angle decreases. This adaptation is necessary to maintain the SINR of the NTN UE by reducing the bandwidth allocated to some UEs to cope with the decreasing received signal power.

Observation 11: As the elevation angle decreases, the proposed mechanism would adaptively increase the NTN group's threshold, i.e., $\boldsymbol{\delta}^N$, reducing UE's bandwidth to adjust to increased propagation loss.

Fig. 13 presents the BS classification results of the proposed mechanisms at different elevation angles. As the elevation angle decreases, the proposed mechanism adaptively decreases

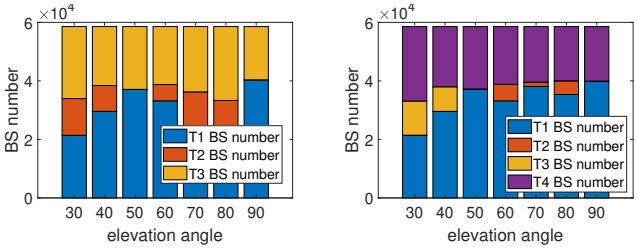

(a) Group sharing M=3 (b) Group sharing M=4

Fig. 13. The trend of TN BS classification results versus elevation angles. Group sharing decreases the BS group's threshold $\boldsymbol{\delta}^T$ as the elevation angle decreases.

the threshold of the BS group, denoted by $\boldsymbol{\delta}^T$, to reduce the aggregated interference and maintain the NTN throughput.

Observation 12: As the elevation angle decreases, the proposed mechanism adaptively decreases the BS group's threshold, i.e., $\boldsymbol{\delta}^T$, lowering the interference to keep NTN's SINR at the desired levels.

XI. Conclusions

This research focuses on the spectrum sharing between NTN UL and TN DL, specifically emphasizing multiple TN BSs within NTN's extreme coverage. We propose an interference-aware radio resource group sharing mechanism to optimize the overall capacity. To achieve a proportional fairness solution between NTN and TN, we present a utility function considering the NTN UL throughput and the available TN DL bandwidth. Since the allocation of radio resource groups is formulated as non-linear integer programming, it becomes intractable due to the sheer number of TN BSs, which amounts to tens of thousands. To address this challenge, we present UE and BS optimal grouping conditions that help to reduce variable numbers. As a result, the resource group allocation problem is transformed into solvable non-linear programming by the UE and BS optimal grouping conditions. Through simulation, we verify the effectiveness of the proposed group sharing and provide insights into resource allocation in the mechanism versus elevation angles, and demonstrate the feasibility of NTN-TN spectrum sharing.

Appendix A
Proof of Theorem 1

Proof. Suppose $N^a_1, ..., N^a_{M-1}$ are parts of a optimal solution to problem $(\boldsymbol{P})$, and $P^a_x \geq P^a_y$ for some $x \in N^a_j, y \in N^a_{j+1}$. We first define NTN throughput changes function representing the NTN throughput changes of moving a UE from group N^a_j to N^a_{j+1} concerning the UE's received power.

$$f(x) = b_{j+1} log(1 + \frac{x}{\sum_{i=1}^{j} I^{T_i, N^a_{j+1}} + I^{T_{j+1}, N^a_{j+1}}}) - b_j log(1 + \frac{x}{\sum_{i=1}^{j} I^{T_i, N^a_j}}) \tag{41}$$

© 2024 IEEE. Personal use of this material is permitted. Permission from IEEE must be obtained for all other uses, in any current or future media, including reprinting/republishing this material for advertising or promotional purposes, creating new collective works, for resale or redistribution to servers or lists, or reuse of any copyrighted component of this work in other works.

Since $x \in N_j^a$ and $y \in N_{j+1}^a$ is a part of a optimal solution, we know $f(P_x^a) \leq 0$ and $f(P_y^a) \geq 0$, respectively. The first derivative of function $f(x)$ is expressed.

$$f^{'}(x) = \frac{b_{j+1}}{\sum_{i=1}^{j} I^{T_i,N_{j+1}^a} + I^{T_{j+1},N_{j+1}^a} + x} - \frac{b_j}{\sum_{i=1}^{j} I^{T_i,N_j^a} + x} \tag{42}$$

Moving a UE from group N_j^a to N_{j+1}^a could increase NTN throughput only when $f^{'}(x) > 0$. Thus, a received power threshold can be derived.

$$x \geq \frac{b_j \sum_{i=1}^{j} I^{T_i,N_{j+1}^a} + I^{T_{j+1},N_{j+1}^a} - b_{j+1} \sum_{i=1}^{j} I^{T_i,N_j^a}}{b_{j+1} - b_j} = \sigma \tag{43}$$

(43) implies that $f(x)$ is an increasing function when $x \geq \sigma$. Since $f(P_y^a) \geq 0$, we know $P_y^a \geq \sigma$. Because $P_x^a \geq P_y^a$, we get $f(P_x^a) > 0$ which contradicts $x \in N_j^a$ is part of the optimal solution. Thus, the theorem is proved by contradiction. □

APPENDIX B
PROOF OF THEOREM 2

Proof. Suppose $T_1, ..., T_M$ are parts of a optimal solution to problem (P), and $S_{a,x}^r \geq S_{a,y}^r$ for some $x \in T_m, y \in T_{m+1}$. According to the relationship between (10), (12), and (13), we first define $\Gamma_k^{N_m^a} := f(\frac{1}{\sum_{n=1}^{m} I^{T_n,N_m^a}})$, where $f(x)$ is a monotonic increasing function.

Let N_m^{a*} be the NTN group m interfered by the new grouping solution that

$$T_m^* = \{T_m \setminus x\} \cup y, \quad T_{m+1}^* + = \{T_{m+1} \setminus y\} \cup x. \tag{44}$$

Let $\Gamma_k^{N_m^{a*}}$ represents the NTN throughput of NTN group m in the new grouping solution T_m^*, T_{m+1}^*.

$$\begin{aligned}
&\Gamma_k^{N_m^{a*}} := f(\frac{1}{\sum_{n=1}^{m-1} I^{T_n,N_m^a} + I^{\{T_m \setminus x\} \cup y,N_m^a}}) \\
&\because I^{T_m,N_m^a} > I^{\{T_m \setminus x\} \cup y,N_m^a} \therefore \Gamma_k^{N_m^a} = f(\frac{1}{\sum_{n=1}^{m} I^{T_n,N_m^a}}) \leq \\
&f(\frac{1}{\sum_{n=1}^{m-1} I^{T_n,N_m^a} + I^{\{T_m \setminus x\} \cup y,N_m^a}}) = \Gamma_k^{N_m^{a*}}
\end{aligned} \tag{45}$$

Thus, we have proved $\Gamma_k^{N_m^a} \leq \Gamma_k^{N_m^{a*}}$.

$$\begin{aligned}
&(\frac{1}{N_{BS}} \sum_{j=1}^{M} \sum_{i \in T_j} \sum_{k=j}^{M} B_k)(\sum_{j=1}^{M-1} \sum_{k \in N_j^a} \Gamma_k^{N_j^a}) \\
&= \frac{1}{N_{BS}}(\sum_{j=1, j \neq \{m,m+1\}}^{M} \sum_{i \in T_j} \sum_{k=j}^{M} B_k + \sum_{i \in T_m} \sum_{k=m}^{M} B_k + \\
&\sum_{i \in T_{m+1}} \sum_{k=m+1}^{M} B_k)(\sum_{j=1, j \neq m}^{M-1} \sum_{k \in N_j^a} \Gamma_k^{N_j^a} + \Gamma_k^{N_m^a}) \\
&\leq \frac{1}{N_{BS}}(\sum_{j \neq m, m+1}^{M} \sum_{i \in T_j} \sum_{k=j}^{M} B_k + \sum_{i \in \{T_m \setminus x\} \cup y} \sum_{k=m}^{M} B_k + \\
&\sum_{i \in \{T_{m+1} \setminus y\} \cup x} \sum_{k=m+1}^{M} B_k)(\sum_{j=1, j \neq m}^{M-1} \sum_{k \in N_j^a} \Gamma_k^{N_j^a} + \Gamma_k^{N_m^{a*}})
\end{aligned} \tag{46}$$

Therefore, T_m and T_{m+1} are not parts of a optimal solution to problem $(\boldsymbol{P})$. The first case is proved by contradiction. □

REFERENCES

[1] D. Peng, D. He, Y. Li, and Z. Wang, "Integrating Terrestrial and Satellite Multibeam Systems Toward 6G: Techniques and Challenges for Interference Mitigation," *IEEE Wireless Communications*, vol. 29, no. 1, pp. 24–31, 2022.

[2] Z. Hassan, E. Heeren-Moon, J. Sabzehali, V. K. Shah, C. Dietrich, J. H. Reed, and E. W. Burger, "Spectrum Sharing of the 12 GHz Band with Two-way Terrestrial 5G Mobile Services: Motivations, Challenges, and Research Road Map," *IEEE Communications Magazine*, pp. 1–7, 2023.

[3] H.-W. Lee, A. Medles, V. Jie, D. Lin, X. Zhu, I.-K. Fu, and H.-Y. Wei, "Reverse Spectrum Allocation for Spectrum Sharing between TN and NTN," in *2021 IEEE Conference on Standards for Communications and Networking (CSCN)*, 2021, pp. 1–6.

[4] X. Zhang, D. Guo, K. An, G. Zheng, S. Chatzinotas, and B. Zhang, "Auction-Based Multichannel Cooperative Spectrum Sharing in Hybrid Satellite-Terrestrial IoT Networks," *IEEE Internet of Things Journal*, vol. 8, no. 8, pp. 7009–7023, 2021.

[5] Y. Ruan, Y. Li, C.-X. Wang, and R. Zhang, "Energy Efficient Adaptive Transmissions in Integrated Satellite-Terrestrial Networks With SER Constraints," *IEEE Transactions on Wireless Communications*, vol. 17, no. 1, pp. 210–222, 2018.

[6] J. Du, C. Jiang, H. Zhang, Y. Ren, and M. Guizani, "Auction Design and Analysis for SDN-Based Traffic Offloading in Hybrid Satellite-Terrestrial Networks," *IEEE Journal on Selected Areas in Communications*, vol. 36, no. 10, pp. 2202–2217, 2018.

[7] P. K. Sharma, P. K. Upadhyay, D. B. da Costa, P. S. Bithas, and A. G. Kanatas, "Performance Analysis of Overlay Spectrum Sharing in Hybrid Satellite-Terrestrial Systems With Secondary Network Selection," *IEEE Transactions on Wireless Communications*, vol. 16, no. 10, pp. 6586–6601, 2017.

[8] S. Vassaki, M. I. Poulakis, A. D. Panagopoulos, and P. Constantinou, "Power Allocation in Cognitive Satellite Terrestrial Networks with QoS Constraints," *IEEE Communications Letters*, vol. 17, no. 7, pp. 1344–1347, 2013.

[9] P. Wang, J. Zhang, X. Zhang, Z. Yan, B. G. Evans, and W. Wang, "Convergence of Satellite and Terrestrial Networks: A Comprehensive Survey," *IEEE Access*, vol. 8, pp. 5550–5588, 2020.

[10] S. Chan, H. Lee, S. Kim, and D. Oh, "Intelligent Low Complexity Resource Allocation Method for Integrated Satellite-Terrestrial Systems," *IEEE Wireless Communications Letters*, vol. 11, no. 5, pp. 1087–1091, 2022.

[11] D. Peng, A. Bandi, Y. Li, S. Chatzinotas, and B. Ottersten, "Hybrid Beamforming, User Scheduling, and Resource Allocation for Integrated Terrestrial-Satellite Communication," *IEEE Transactions on Vehicular Technology*, vol. 70, no. 9, pp. 8868–8882, 2021.

[12] Y. Cho, W. Yang, D. Oh, and H.-S. Jo, "Multi-Agent Deep Reinforcement Learning for Interference-Aware Channel Allocation in Non-Terrestrial Networks," *IEEE Communications Letters*, vol. 27, no. 3, pp. 936–940, 2023.

[13] E. Lagunas, S. K. Sharma, S. Maleki, S. Chatzinotas, and B. Ottersten, "Resource Allocation for Cognitive Satellite Communications With Incumbent Terrestrial Networks," *IEEE Transactions on Cognitive Communications and Networking*, vol. 1, no. 3, pp. 305–317, 2015.

[14] W. Wang, S. Zhao, Y. Zheng, and Y. Li, "Resource Allocation Method of Cognitive Satellite Terrestrial Networks Under Non-Ideal Spectrum Sensing," *IEEE Access*, vol. 7, pp. 7957–7964, 2019.

[15] L. Wang, F. Li, X. Liu, K.-Y. Lam, Z. Na, and H. Peng, "Spectrum Optimization for Cognitive Satellite Communications With Cournot Game Model," *IEEE Access*, vol. 6, pp. 1624–1634, 2018.

[16] Z. Chen, D. Guo, G. Ding, X. Tong, H. Wang, and X. Zhang, "Optimized Power Control Scheme for Global Throughput of Cognitive Satellite-Terrestrial Networks Based on Non-Cooperative Game," *IEEE Access*, vol. 7, pp. 81 652–81 663, 2019.

[17] Y. Ruan, Y. Li, C.-X. Wang, R. Zhang, and H. Zhang, "Energy Efficient Power Allocation for Delay Constrained Cognitive Satellite Terrestrial Networks Under Interference Constraints," *IEEE Transactions on Wireless Communications*, vol. 18, no. 10, pp. 4957–4969, 2019.

[18] X. Wen, Y. Ruan, Y. Li, and R. Zhang, "Cognitive Region Design for Overlay Cognitive Satellite Terrestrial Networks," *IEEE Communications Letters*, vol. 25, no. 1, pp. 244–248, 2021.

[19] H. Niu, Z. Lin, K. An, X. Liang, Y. Hu, D. Li, and G. Zheng, "Active RIS-Assisted Secure Transmission for Cognitive Satellite Terrestrial Networks," *IEEE Transactions on Vehicular Technology*, vol. 72, no. 2, pp. 2609–2614, 2023.

© 2024 IEEE. Personal use of this material is permitted. Permission from IEEE must be obtained for all other uses, in any current or future media, including reprinting/republishing this material for advertising or promotional purposes, creating new collective works, for resale or redistribution to servers or lists, or reuse of any copyrighted component of this work in other works.

[20] Y. Zhang, H. Zhang, H. Zhou, K. Long, and G. K. Karagiannidis, "Resource Allocation in Terrestrial-Satellite-Based Next Generation Multiple Access Networks With Interference Cooperation," *IEEE Journal on Selected Areas in Communications*, vol. 40, no. 4, pp. 1210–1221, 2022.
[21] Z. Lin, M. Lin, J.-B. Wang, T. de Cola, and J. Wang, "Joint Beamforming and Power Allocation for Satellite-Terrestrial Integrated Networks With Non-Orthogonal Multiple Access," *IEEE Journal of Selected Topics in Signal Processing*, vol. 13, no. 3, pp. 657–670, 2019.
[22] S. Xie, B. Zhang, D. Guo, and B. Zhao, "Performance Analysis and Power Allocation for NOMA-Based Hybrid Satellite-Terrestrial Relay Networks With Imperfect Channel State Information," *IEEE Access*, vol. 7, pp. 136 279–136 289, 2019.
[23] L. Wang, Y. Wu, H. Zhang, S. Choi, and V. C. M. Leung, "Resource Allocation for NOMA Based Space-Terrestrial Satellite Networks," *IEEE Transactions on Wireless Communications*, vol. 20, no. 2, pp. 1065–1075, 2021.
[24] X. Fang, W. Feng, Y. Wang, Y. Chen, N. Ge, Z. Ding, and H. Zhu, "NOMA-Based Hybrid Satellite-UAV-Terrestrial Networks for 6G Maritime Coverage," *IEEE Transactions on Wireless Communications*, vol. 22, no. 1, pp. 138–152, 2023.
[25] Q. Gao, M. Jia, Q. Guo, X. Gu, and L. Hanzo, "Jointly Optimized Beamforming and Power Allocation for Full-Duplex Cell-Free NOMA in Space-Ground Integrated Networks," *IEEE Transactions on Communications*, vol. 71, no. 5, pp. 2816–2830, 2023.
[26] 3GPP, "Study on New Radio (NR) to support non-terrestrial networks," 3rd Generation Partnership Project (3GPP), Technical report (TR) 38.811, 10 2020, version 15.4.0.
[27] ——, "Solutions for NR to support Non-Terrestrial Networks (NTN)," 3rd Generation Partnership Project (3GPP), Technical report (TR) 38.821, 06 2021, version 16.1.0.
[28] ——, "Non-terrestrial networks (NTN) related RF and co-existence aspects," 3rd Generation Partnership Project (3GPP), Technical report (TR) 38.863, 06 2022, version 17.0.0.
[29] ——, "Study on new radio access technology: Radio Frequency (RF) and co-existence aspects," 3rd Generation Partnership Project (3GPP), Technical report (TR) 38.803, 04 2022, version 14.3.0.
[30] ——, "Study on channel model for frequencies from 0.5 to 100 GHz," 3rd Generation Partnership Project (3GPP), Technical report (TR) 38.901, 03 2022, version 17.0.0.
[31] R. Liu, K. Guo, K. An, Y. Huang, F. Zhou, and S. Zhu, "Resource Allocation for Cognitive Satellite-HAP-Terrestrial Networks With Non-Orthogonal Multiple Access," *IEEE Transactions on Vehicular Technology*, pp. 1–5, 2023.

Hao-Wei Lee received the B.S. degree in Electrical Engineering and Computer Science Undergraduate Honors Program and the M.S. degree in Institute of Communications Engineering from National Chiao Tung University in 2015 and 2017, respectively. He is currently working toward the Ph.D. degree in communication engineering with the Graduate Institute of Communication Engineering from National Taiwan University. He was an Intern with MediaTek from 2020 to 2022. His research includes NTN, spectrum sharing, interference mitigation, as well as 3GPP NR standards.

Chun-Chia Chen received B.S., M.S., and Ph.D. degrees in Computer Science from National Tsing Hua University (NTHU), Taiwan, in 1999, 2001, and 2007. He currently worked as a senior engineer in MediaTek. He actively participates in 5G mobile communication,6G mobile communication, artificial satellites, cellular radio, millimeter wave communication, satellite communication, and telecommunication traffic.

Stephanie Liao is a senior engineer within the Advance Communication Technology division at MediaTek. She studied her bachelor's at The University of Auckland and worked at Vodafone New Zealand as a RAN Devops Engineer until 2019, with core involvement in their national 5G cellular deployment strategy and feature deployment. She then acquired her Master's in Wireless Communications, class of 2021 at University College London, with an internship at Viavi Wireless Solutions and joined MediaTek towards the end of 2021, primarily focusing on NTN research and system design.

Abdelkader Medles is a Senior Technical Manager at MediaTek. He earned his PhD in electrical engineering from Telecom Paris while working on advanced signal processing and information theory for MIMO systems in 2004. He worked as a research and teaching assistant at Institute Eurecom from 2000 to 2004, then as a post-doctoral researcher at Bell Labs Lucent from 2004 to 2006. He then worked in research and development of the physical layer for 3GPP WCDMA, LTE and 5G standards successively in Icera Semiconductor, Mstar and MediaTek. Since he joined MediaTek in 2014 he led an algorithm and architecture team for the design of the user equipment modem and contributed to the definition of 5G specifications as a research team leader and 3GPP delegate. He also led a proof-of-concept research and prototyping team for 5G NTN technology. His current research interests span non-terrestrial networks and 6G wireless systems.

Debby Lin is a senior technical manager at MediaTek Inc. She received her Ph.D. degree in communication engineering from National Chiao Tung University, Taiwan in 2009. In 2007 and 2008, she was a visiting scholar at RWTH Aachen University and the University of Washington, respectively. She joined MediaTek in 2010 and has been working in the advanced communication technology division. Throughout her career, she has served as the technical lead in MediaTek's NTN research and development, responsible for system design, prototyping, system integration and verification, and technical promotion.

I-Kang Fu is a senior director of technology at MediaTek advanced communication technology division. He received the Ph.D degree from National Chiao Tung University, Taiwan in 2007, and then joined MediaTek since 2008 until now. Since 2005, He has been actively developing and contributing new technology to mobile cellular standardization projects in IEEE and 3GPP for mobile WiMAX, LTE, NB-IoT and 5G NR. He has been leading MediaTek's NTN R&D initiatives from research, prototype, standardization and ecosystem engagement, now he also leads MediaTek's advanced communication technology development for B5G and 6G. He has served as Chair position for Taiwan standard organization (TAICS) TC1 since 2018.

Hung-Yu Wei (Senior Member, IEEE) received the B.S. degree in electrical engineering from National Taiwan University, in 1999, and the M.S. and Ph.D. degrees in electrical engineering from Columbia University, in 2001 and 2005. In July 2005, he joined the Department of Electrical Engineering, National Taiwan University. He is a Professor with the Graduate Institute of Communication Engineering, Department of Electrical Engineering, National Taiwan University. He actively participates in wireless communications standardization activities. His research interests include broadband wireless communications, vehicular networking, cross-layer design for wireless multimedia communications, Internet of Things, and game theoretic models for networking. From 2008 to 2009, he was a Consulting Member of the Acts and Regulation Committee of the National Communications Commission. He was the Chair of the IEEE Vehicular Technology Society Taipei Chapter. He is the Chair of the IEEE 1935 standard working group on Edge/Fog Manageability and Orchestration.

© 2024 IEEE. Personal use of this material is permitted. Permission from IEEE must be obtained for all other uses, in any current or future media, including reprinting/republishing this material for advertising or promotional purposes, creating new collective works, for resale or redistribution to servers or lists, or reuse of any copyrighted component of this work in other works.